

EmbedDistill: A Geometric Knowledge Distillation for Information Retrieval

Seungyeon Kim, Ankit Singh Rawat, Manzil Zaheer,
 Sadeep Jayasumana, Veeranjaneyulu Sadhanala, Wittawat Jitkrittum,
 Aditya Krishna Menon, Rob Fergus, Sanjiv Kumar

Google LLC, USA

{seungyeon,ankitsrawat,manzilzaheer}@google.com
 {sadeep,veerus,wittawat,adityakmenon,robfergus,sanjivk}@google.com

Abstract

Large neural models (such as Transformers) achieve state-of-the-art performance for information retrieval (IR). In this paper, we aim to improve distillation methods that pave the way for the deployment of such models in practice. The proposed distillation approach supports both retrieval and re-ranking stages and crucially leverages the relative geometry among queries and documents learned by the large teacher model. It goes beyond existing distillation methods in the IR literature, which simply rely on the teacher’s scalar scores over the training data, on two fronts: providing stronger signals about local geometry via embedding matching and attaining better coverage of data manifold globally via query generation. Embedding matching provides a stronger signal to align the representations of the teacher and student models. At the same time, query generation explores the data manifold to reduce the discrepancies between the student and teacher where training data is sparse. Our distillation approach is theoretically justified and applies to both dual encoder (DE) and cross-encoder (CE) models. Furthermore, for distilling a CE model to a DE model via embedding matching, we propose a novel dual pooling-based scorer for the CE model that facilitates a distillation-friendly embedding geometry, especially for DE student models.

1 Introduction

Neural models for information retrieval (IR) are increasingly used to model the true ranking function in various applications, including web search [Mitra and Craswell, 2018], recommendation [Zhang et al., 2019], and question-answering (QA; Chen et al. 2017). Notably, the recent success of Transformers [Vaswani et al., 2017]-based pre-trained language models [Devlin et al., 2019, Liu et al., 2019, Raffel et al., 2020] on a wide range of natural language understanding tasks has also prompted their utilization in IR to capture query-document relevance [see, e.g., Dai and Callan, 2019b, MacAvaney et al., 2019a, Nogueira and Cho, 2019, Lee et al., 2019, Karpukhin et al., 2020a].

A typical IR system comprises two stages: (1) A *retriever* first selects a small subset of potentially relevant candidate documents (out of a large collection) for a given query; and (2) A *re-ranker* then identifies a precise ranking among the candidates provided by the retriever. *Dual-encoder* (DE) models are the de-facto architecture for retrievers [Lee et al., 2019, Karpukhin et al., 2020a]. Such models independently embed queries and documents into a common space, and capture their relevance by simple operations on these embeddings such as the inner product. This enables offline creation of a document index and supports fast retrieval during inference via efficient maximum inner product search (MIPS) implementations [Guo et al.,

2020, Johnson et al., 2021], with *online* query embedding generation primarily dictating the inference latency. *Cross-encoder* (CE) models, on the other hand, are preferred as re-rankers, owing to their excellent performance [Nogueira and Cho, 2019, Dai and Callan, 2019a, Yilmaz et al., 2019]. A CE model jointly encodes a query-document pair while enabling early interaction among query and document features. Employing a CE model for retrieval is often infeasible, as it would require processing a given query with *every* document in the collection at inference time. In fact, even in the re-ranking stage, the inference cost of CE models is high enough [Khattab and Zaharia, 2020] to warrant exploration of efficient alternatives [Hofstätter et al., 2020, Khattab and Zaharia, 2020, Menon et al., 2022].

Knowledge distillation [Bucilă et al., 2006, Hinton et al., 2015] provides a general strategy to address the prohibitive inference cost associated with high-quality large neural models. In the IR literature, most existing distillation methods only rely on the teacher’s query-document relevance scores [see, e.g., Lu et al., 2020, Hofstätter et al., 2020, Chen et al., 2021, Ren et al., 2021, Santhanam et al., 2021] or their proxies [Izacard and Grave, 2021]. However, given that neural IR models are inherently embedding-based, it is natural to ask: *Is it useful to go beyond matching of the teacher and student models’ scores, and directly aim to align their embedding spaces?*

With this in mind, we propose a novel distillation method for IR models that utilizes an *embedding matching* task to train the student. The proposed method supports *cross-architecture distillation* and improves upon existing distillation methods for both retriever and re-ranker models. When distilling a large DE model into a smaller DE model, for a given query (document), one can minimize the distance between the query (document) embeddings of the teacher and student after compatible projection layers to account for any dimensionality mismatch. In contrast, defining an embedding matching task for distilling a CE model into a DE model is not as straightforward. For Transformers-based CE models, it is common to use the final embedding of a special token, e.g., [CLS] in BERT [Devlin et al., 2019], to compute query-document relevance [Nogueira and Cho, 2019]. However, as we note in Sec. 4.2, this token embedding does not capture semantic similarity between the query and document. To make CE models more amenable to distillation via embedding matching, we propose a modified CE scoring approach by utilizing a novel *dual-pooling* strategy: this separately pools the final query and document token embeddings, and then computes the inner product between the pooled embeddings as the relevance score. Our key contributions toward improving IR models via distillation are:

- We propose a novel distillation approach for neural IR models, namely `EmbedDistill`, that goes beyond score matching and aligns the embedding spaces of the teacher and student models.
- We consider a novel DE to DE distillation setup to showcase the effectiveness of `EmbedDistill` (Sec. 4.1). Specifically, we consider a student DE model with an *asymmetric* configuration, consisting of a small query encoder and a *frozen* document encoder inherited from the teacher. This configuration significantly reduces inference latency of query embedding generation, while leveraging the teachers’ high-quality document index.
- We show that `EmbedDistill` can leverage synthetic data to improve a student by further aligning the embedding spaces of the teacher and student (Sec. 4.3).
- We theoretically justify both embedding matching and query generation components of our proposed method (Sec. 5). Further, we provide a comprehensive empirical evaluation of the method (Sec. 6) on two standard IR benchmarks – Natural Questions [Kwiatkowski et al., 2019a] and MSMARCO [Nguyen et al., 2016]. Additionally, we also evaluate `EmbedDistill` on BEIR benchmark [Thakur et al., 2021] which is used to measure the zero-shot performance of an IR model.
- Finally, we demonstrate the utility of embedding matching for CE to DE distillation on MSMARCO by employing a novel pooling strategy, namely *dual pooling* (Sec. 4.2), which may be of independent interest.

2 Related work

Here, we review some existing Transformers-based IR models, and discuss prior work on distillation and data augmentation for such models. We also cover prior efforts on aligning representations during distillation for *non-IR* settings. Unlike our problem setting where the DE student is factorized, these works mainly consider distilling a single large Transformer into a smaller one.

Transformers-based architectures for IR. Besides DE and CE models described in Sec. 1, intermediate configurations [MacAvaney et al., 2020, Khattab and Zaharia, 2020, Nie et al., 2020, Luan et al., 2021] have been proposed. Such models independently encode query and document before applying a more complex *late interaction* between the two. Interestingly, Nogueira et al. [2020] explore generative encoder-decoder style model for re-ranking, where a T5 [Raffel et al., 2020] model takes a query-document pair as input and its score for certain target tokens (e.g., True/False) defines the relevance score for the pair. In this paper, we focus on basic DE and CE models to showcase the benefits of our proposed geometric distillation approach. Exploring embedding matching for other aforementioned architectures is an interesting avenue for future exploration.

Distillation for IR. Traditional distillation techniques have been widely applied in the IR literature, often to distill a teacher CE model to a student DE model [Li et al., 2020, Chen et al., 2021]. Recently, distillation from a DE model (with complex late interaction) to another DE model (with inner-product scoring) has also been considered [Lin et al., 2021, Hofstätter et al., 2021]. As for distilling across different model architectures, Lu et al. [2020], Izacard and Grave [2021] consider distillation from a teacher CE model to a student DE model. Hofstätter et al. [2020] conduct an extensive study of knowledge distillation across a wide-range of model architectures. Most existing distillation schemes for IR rely on only teacher scores; by contrast, we propose a geometric approach that also utilizes the teacher *embeddings*. Many recent efforts [Qu et al., 2021, Ren et al., 2021, Santhanam et al., 2021] show that iterative multi-stage (self-)distillation improves upon single-stage distillation [Qu et al., 2021, Ren et al., 2021, Santhanam et al., 2021]. These approaches use a model from the previous stage to obtain labels [Santhanam et al., 2021] as well as mine harder-negatives [Xiong et al., 2021]. We only focus on the single-stage distillation in this paper. Multi-stage procedures are complementary to our work, as one can employ our proposed embedding-matching approach in various stages of such a procedure. Interestingly, we demonstrate in Sec. 6 that our proposed EmbedDistill can successfully benefit from high quality models trained with such complex procedures [Reimers et al., 2019, Zhang et al., 2022]. In particular, our single-stage distillation method can transfer almost all of their performance gains to even smaller models. Also to showcase that our method brings gain orthogonal to how teacher was trained, we conduct experiments with single-stage trained teacher in Appendix F.5.

Distillation with representation alignments. Outside of the IR context, a few prior works proposed to utilize alignment between hidden layers during distillation [Romero et al., 2014, Sanh et al., 2019, Jiao et al., 2020, Aguilar et al., 2020, Zhang and Ma, 2020]. Chen et al. [2022] utilize the representation alignment to re-use teacher’s classification layer. Our work differs from these as it needs to address multiple challenges presented by an IR setting: 1) cross-architecture distillation such as CE to DE distillation; 2) partial representation alignment of query or document representations as opposed to aligning for the entire input, i.e., a query-documents pair; 3) catering representation alignment approach to novel IR setups such as asymmetric DE configuration; and 4) dealing with negative sampling due to a large number of classes (documents). To the best of our knowledge, our work is first in the IR literature that goes beyond simply matching scores (or its proxies).

Semi-supervised learning for IR. Data augmentation or semi-supervised learning has been previously used to ensure data efficiency in IR [see, e.g., MacAvaney et al., 2019b, Zhao et al., 2021]. More interestingly, data augmentation via large pre-trained models have enabled performance improvements as well.

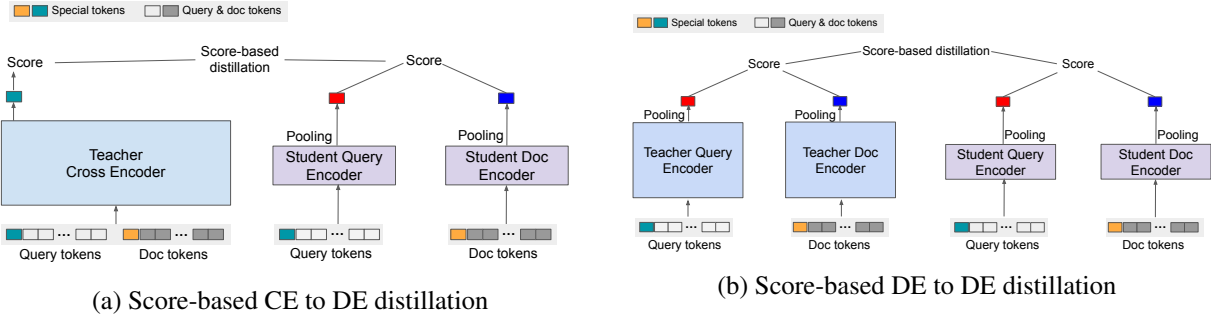


Figure 1: Illustration of score-based distillation for IR (cf. Section 3.2). Fig. 1a describes distillation from a teacher [CLS]-pooled CE model to a student DE model. Fig. 1b depicts distillation from a teacher DE model to a student DE model. Here, both distillation setup employ symmetric DE configurations where query and document encoders of the student model are of the same size.

Doc2query [Nogueira et al., 2019b,a] performs document expansion by generating queries that are relevant to the document and appending those queries to the document. Query expansion has also been considered, e.g., for document re-ranking [Zheng et al., 2020]. Notably, generating synthetic (query, passage, answer) triples from a text corpus to augment existing training data for QA systems also leads to significant gains [Alberti et al., 2019, Oğuz et al., 2021]. Furthermore, even zero-shot approaches, where no labeled query-document pairs are used, can also perform competitively to supervised methods. Such methods train a DE model by relying on inverse cloze task [Lee et al., 2019, Izacard et al., 2021], synthetic query-document pairs given a target text corpus [Ma et al., 2021], or relevance scores from large pretrained models [Sachan et al., 2022]. Unlike these works, we utilize query-generation capability to ensure tighter alignment between the embedding spaces of the teacher and student.

3 Background

Let \mathcal{Q} and \mathcal{D} denote the query and document spaces, respectively. An IR model is equivalent to a scorer $s : \mathcal{Q} \times \mathcal{D} \rightarrow \mathbb{R}$, i.e., it assigns a (relevance) score $s(q, d)$ for a query-document pair $(q, d) \in \mathcal{Q} \times \mathcal{D}$. Ideally, we want to learn an IR model or scorer that is faithful to the true query-document relevance, i.e., $s(q, d) > s(q, d')$ iff the document d is more relevant to the query q than document d' . We assume access to n labeled training examples $\mathcal{S}_n = \{(q_i, \mathbf{d}_i, \mathbf{y}_i)\}_{i \in [n]}$. Here, $\mathbf{d}_i = (d_{i,1}, \dots, d_{i,L}) \in \mathcal{D}^L$, $\forall i \in [n]$, denotes a list of L documents and $\mathbf{y}_i = (y_{i,1}, \dots, y_{i,L}) \in \{0, 1\}^L$ denotes the corresponding labels such that $y_{i,j} = 1$ iff the document $d_{i,j}$ is relevant to the query q_i . Given \mathcal{S}_n , we learn an IR model by minimizing

$$R(s; \mathcal{S}_n) := \frac{1}{n} \sum_{i \in [n]} \ell(s_{q_i, \mathbf{d}_i}, \mathbf{y}_i), \quad (1)$$

where $s_{q_i, \mathbf{d}_i} := (s(q_i, d_{1,1}), \dots, s(q_i, d_{1,L}))$ and, accordingly, $\ell(s_{q_i, \mathbf{d}_i}, \mathbf{y}_i)$ denotes the loss s incurs on $(q_i, \mathbf{d}_i, \mathbf{y}_i)$. We defer concrete choices for the loss function ℓ to Appendix A.

While this learning framework is general enough to work with any IR models as the scorers, next, we formally introduce two families of Transformer-based IR models that are prevalent in the recent literature.

3.1 Transformer-based IR models: Cross-encoders and Dual-encoders

Let query $q = (q^1, \dots, q^{m_1})$ and document $d = (d^1, \dots, d^{m_2})$ consist of m_1 and m_2 tokens, respectively. We now discuss how Transformers-based CE and DE models process a the (q, d) pair.

Cross-encoder model. Let $p = [q; d]$ be the sequence obtained by concatenating q and d . Further, let \tilde{p} be the sequence obtained by adding special tokens such $[\text{CLS}]$ and $[\text{SEP}]$ to p . Given an encoder-only Transformer model Enc , the relevance score for the (q, d) pair is

$$s(q, d) = \langle w, \text{pool}(\text{Enc}(\tilde{p})) \rangle = \langle w, \text{emb}_{q,d} \rangle, \quad (2)$$

where w is a d -dimensional classification vector, and $\text{pool}(\cdot)$ denotes a pooling operation that transforms the contextualized token embeddings $\text{Enc}(\tilde{p})$ to a joint embedding vector $\text{emb}_{q,d}^t$. $[\text{CLS}]$ -pooling is a common operation that simply outputs the embedding of the $[\text{CLS}]$ token as $\text{emb}_{q,d}^t$.

Dual-encoder model. Let \tilde{q} and \tilde{d} be the sequences obtained by adding appropriate special tokens to q and d , respectively. A DE model comprises two (encoder-only) Transformers Enc_Q and Enc_D , which we call query and document encoders, respectively.¹ Let $\text{emb}_q = \text{pool}(\text{Enc}_Q(\tilde{q}))$ and $\text{emb}_d = \text{pool}(\text{Enc}_D(\tilde{d}))$ denote the query and document embeddings, respectively. Now, one can define $s(q, d) = \langle \text{emb}_q, \text{emb}_d \rangle$ to be the relevance score assigned to the (q, d) pair by the DE model.

3.2 Score-based distillation for IR models

Most distillation schemes for IR [e.g., Lu et al., 2020, Hofstätter et al., 2020, Chen et al., 2021] rely on teacher relevance scores (cf. Fig. 1). In particular, given a training set \mathcal{S}_n and a teacher with scorer s^t , one learns a student with scorer s^s by minimizing

$$R(s^s, s^t; \mathcal{S}_n) = \frac{1}{n} \sum_{i \in [n]} \ell_d(s_{q,d_i}^s, s_{q,d_i}^t), \quad (3)$$

where ℓ_d captures the discrepancy between s^s and s^t . See Appendix A for common choices for ℓ_d .

4 Embedding-matching based distillation

Since modern neural IR models are inherently embedding-based, we propose to explicitly align the embedding spaces of the teacher and student via a novel distillation method, namely **EmbedDistill**. Our proposal goes beyond existing distillation methods in the IR literature that only use the teacher scores. Next, we introduce **EmbedDistill** for two prevalent settings: (1) distilling a large DE model to a smaller DE model;² and (2) distilling a CE model to a DE model.

4.1 DE to DE distillation

Given a (q, d) pair, let emb_q^t and emb_d^t be the query and document embeddings produced by the query encoder Enc_Q^t and document encoder Enc_D^t of the teacher DE model, respectively. Similarly, let emb_q^s and emb_d^s

¹It is common to employ dual-encoder models where query and document encoders are shared.

²We focus on DE to DE distillation setup as the CE to CE distillation is special case of the former with the classification vector w (cf. Eq. 2) being the trivial second encoder.

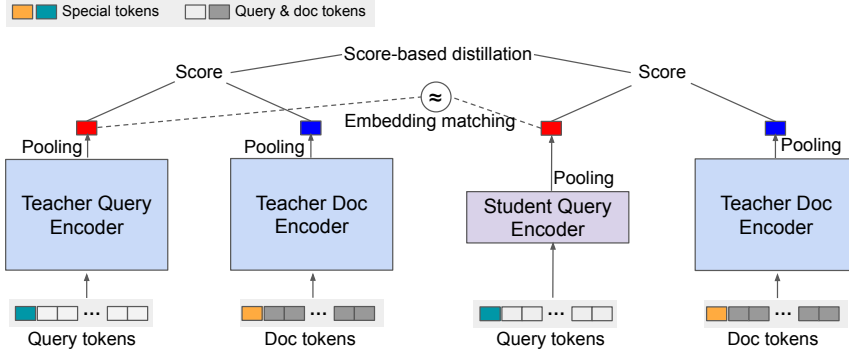


Figure 2: Proposed DE to DE distillation with query embedding matching. The figure describes a setting where student employs an asymmetric DE configuration with a small query encoder and a large (non-trainable) document encoder inherited from the teacher. The smaller query encoder ensures small latency for encoding query during inference, and large document encoder leads to a good quality document index.

denote the query and document embeddings produced by a student DE model with $(\text{Enc}_Q^s, \text{Enc}_D^s)$ as its query and document encoders. Now, EmbedDistill optimizes the following embedding alignment loss in addition to the score-matching loss from Sec. 3.2:

$$R_{\text{Emb}}(\mathbf{t}, \mathbf{s}; \mathcal{S}_n) = \frac{1}{n} \sum_{(q, d) \in \mathcal{S}_n} (\|\mathbf{emb}_q^t - \text{proj}(\mathbf{emb}_q^s)\| + \|\mathbf{emb}_d^t - \text{proj}(\mathbf{emb}_d^s)\|), \quad (4)$$

where proj is an optional trainable layer that is required if the teacher and student produce different sized embeddings. Alternatively, one can employ other variants of EmbedDistill, e.g., focusing on only aligning the query embeddings takes the following form (cf. Fig. 2).

$$R_{\text{Emb}, Q}(\mathbf{t}, \mathbf{s}; \mathcal{S}_n) = \frac{1}{n} \sum_{q \in \mathcal{S}_n} \|\mathbf{emb}_q^t - \text{proj}(\mathbf{emb}_q^s)\|. \quad (5)$$

Asymmetric DE. We also propose a novel student DE configuration where the student employs the teacher’s document encoder (i.e., $\text{Enc}_D^s = \text{Enc}_D^t$) and only train its query encoder, which is much smaller compared to the teacher’s query encoder. For such a setting, it is natural to only employ the embedding matching loss in Eq. 5 as the document embeddings are aligned by design (cf. Fig. 2).

Note that this asymmetric student DE does not incur an increase in latency despite the use of a large teacher document encoder. This is because the large document encoder is only needed to create a good quality document index offline, and only the query encoder is evaluated at inference time. Thus, for DE to DE distillation, we prescribe the asymmetric DE configuration universally. Our theoretical analysis (cf. Sec. 5) and experimental results (cf. Sec. 6) suggest that the ability to inherit the document tower from the teacher DE model can drastically improve the final performance, especially when combined with EmbedDistill.

4.2 CE to DE distillation

Let Enc^t be the (single) teacher CE model encoder, and $(\text{Enc}_Q^s, \text{Enc}_D^s)$ denote the student DE model’s query and document encoders. When distilling from a CE to DE model, defining an effective embedding matching task is not as straightforward as in Sec. 4.1: since CE models jointly encode query-document pairs, it is not obvious how to extract individual query and document embeddings for matching.

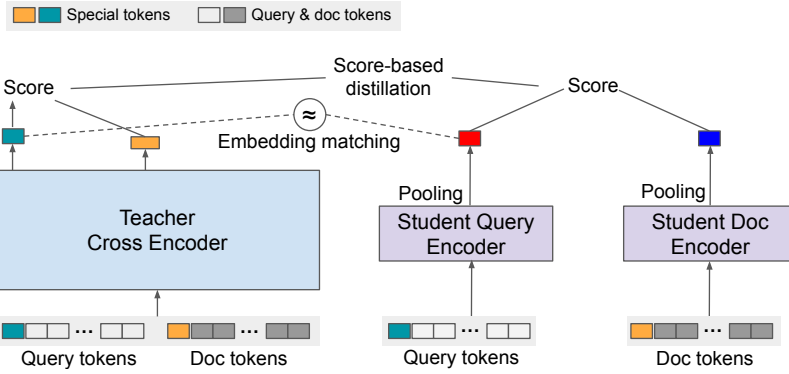


Figure 3: Illustration of CE to DE distillation using EmbedDistill, with CE model employing dual pooling.

As a naïve solution, for a (q, d) pair, one can simply match a joint transformation of the student’s query embedding emb_q^s and document embedding emb_d^s to the teacher’s joint embedding $\text{emb}_{q,d}^t$. However, we observed that including such an embedding matching task often leads to severe over-fitting, and results in a poor student. Since $s^t(q, d) = \langle w, \text{emb}_{q,d}^t \rangle$, during CE model training, the joint embeddings $\text{emb}_{q,d}^t$ for relevant and irrelevant (q, d) pairs are encouraged to be aligned with w and $-w$, respectively. This produces degenerate embeddings that do not capture semantic query-to-document relationships. We notice that even the final query and document token embeddings lose such semantic structure (cf. Appendix G.2). Thus, a teacher CE model with $s^t(q, d) = \langle w, \text{emb}_{q,d}^t \rangle$ does not add value for distillation beyond score-matching; in fact, it *hurts* to include naïve embedding matching. Next, we propose a modified CE model training strategy that facilitates EmbedDistill.

CE models with dual pooling. We propose *dual pooling* to produce two embeddings $\text{emb}_{q \leftarrow (q,d)}^t$ and $\text{emb}_{d \leftarrow (q,d)}^t$ from a CE model that serve as the *proxy* query and document embeddings, respectively. Accordingly, we define the relevance score as $s^t(q, d) = \langle \text{emb}_{q \leftarrow (q,d)}^t, \text{emb}_{d \leftarrow (q,d)}^t \rangle$. We explore two variants of dual pooling: (1) special token-based pooling that pools from `[CLS]` and `[SEP]`; and (2) segment-based weighted mean pooling that separately performs weighted averaging on the query and document segments of the final token embeddings. See Appendix B for details.

In addition to employing the dual pooling, we also utilize a reconstruction loss during the CE training, which measures the likelihood of predicting each token of the original input from the final token embeddings. This loss encourages reconstruction of query and document tokens based on the final token embeddings and prevents the degeneration of the token embeddings during training. Given proxy embeddings from the teacher CE, we can perform EmbedDistill with the embedding matching loss defined in Eq. 4 or Eq. 5 (cf. Fig. 3).

4.3 Task-specific online data generation

Data augmentation as a general technique has been previously considered in the IR literature [see, e.g., Nogueira et al., 2019b, Oğuz et al., 2021, Izacard et al., 2021], especially in data-limited, out-of-domain, or zero-shot settings. As EmbedDistill aims to align the embeddings spaces of the teacher and student, the ability to generate similar queries or documents can naturally help enforce such an alignment globally on the task-specific manifold. Given a set of unlabeled task-specific query and document pairs \mathcal{U}_m , we can further add the embedding-alignment loss $R_{\text{Emb}}(t, s; \mathcal{U}_m)$ to our training objective (cf. Eq.4). Interestingly, for DE to DE distillation setting, our approach can even benefit from a large collection of task-specific queries \mathcal{Q}' or documents \mathcal{D}' . Here, we can independently employ embedding matching losses $R_{\text{Emb},Q}(t, s; \mathcal{Q}')$ (cf. Eq. 5)

and $R_{\text{Emb},D}(t, s; \mathcal{D}')$ that focus on queries and documents, respectively. Please refer to Appendix E for additional details.

5 Improvements in the student generalization

Note that we motivate EmbedDistill as well as asymmetric DE configuration where the student DE model inherits the teacher’s document encoder from their potential ability to ensure a better alignment between the teacher and student embedding spaces. In this section, we provide a theoretical justification for both of these proposals by showing that they indeed result in a better generalization (test-time) performance for the student and reduce the gap between the teacher and the student.

Let $R(s) = \mathbb{E} [\ell(s_{q,d}, y)]$ be the population version of the empirical risk in Eq. 1. Note that $R(s)$ is a measure of the test time performance of the IR model defined by the scorer s . Since we want the student model to (at least) closely approximate the teacher model’s performance, we are interested in bounding $R(s^s) - R(s^t)$, i.e., the gap between the test time performance of the student and teacher models. The following result provides a bound on this quantity (see Appendix C.1 for a formal statement and proof). For simplicity, we focus on $L = 1$ (cf. Sec. 3). The result can be extended to $L > 1$ with more complex notation.

Theorem 5.1 (Teacher-student performance gap (informal)). *Let \mathcal{F} and \mathcal{G} denote the function classes for the query and document encoders for the student model, respectively. Suppose that the score-based distillation loss ℓ_d in Eq. 3 is based on binary cross entropy loss (Eq. 11 in Appendix A). Let one-hot (label-dependent) loss ℓ in Eq. 1 be the binary cross entropy loss (Eq. 9 in Appendix A). Further, assume that all encoders have the same output dimension and embeddings have their ℓ_2 -norm bounded by K . Then, we have*

$$R(s^s) - R(s^t) \leq \mathcal{E}_n(\mathcal{F}, \mathcal{G}) + 2KR_{\text{Emb},Q}(t, s; \mathcal{S}_n) + 2KR_{\text{Emb},D}(t, s; \mathcal{S}_n) + \Delta(s^t; \mathcal{S}_n) + K^2 \left(\mathbb{E} [|\sigma(s_{q,d}^t) - y|] + \frac{1}{n} \sum_{i \in [n]} |\sigma(s_{q_i,d_i}^t) - y_i| \right),$$

where σ denotes the sigmoid function,

$$\mathcal{E}_n(\mathcal{F}, \mathcal{G}) := \sup_{s^s \in \mathcal{F} \times \mathcal{G}} |R(s^s, s^t; \mathcal{S}_n) - \mathbb{E} \ell_d(s_{q,d}^s, s_{q,d}^t)|$$

and $\Delta(s^t; \mathcal{S}_n)$ denotes the deviation between the empirical risk (on \mathcal{S}_n) and population risk of the teacher model s^t .

The last three quantities in our bound on the teacher-student performance gap, namely $\Delta(s^t; \mathcal{S}_n)$, $\mathbb{E} [|\sigma(s_{q,d}^t) - y|]$, and $\frac{1}{n} \sum_{i \in [n]} |\sigma(s_{q_i,d_i}^t) - y_i|$, are independent of the underlying student model. These terms solely depend on the quality of the underlying teacher model s^t .

More importantly, the teacher-student gap can be made small by reducing the following three terms: 1) uniform deviation of the student’s empirical distillation risk from its population version $\mathcal{E}_n(\mathcal{F}, \mathcal{G})$; 2) query embedding matching loss for the student $R_{\text{Emb},Q}(t, s; \mathcal{S}_n)$; and 3) doc embedding matching loss for the student $R_{\text{Emb},D}(t, s; \mathcal{S}_n)$. The last two terms suggest that the teacher-student gap naturally goes down as the embeddings of the student and teacher models become aligned. In particular, when the student inherits the document encoder from the teacher, the third term $R_{\text{Emb},D}(t, s; \mathcal{S}_n)$ vanishes. In general, these last two terms justify EmbedDistill which either employ Eq. 4 or Eq. 5 (when student inherits teacher’s document encoder).

Table 1: *Full* recall performance of various student DE models on NQ dev set, including symmetric DE student model (67.5M or 11.3M transformer for both encoders), and asymmetric DE student model (67.5M or 11.3M transformer as query encoder and document embeddings inherited from the teacher). All distilled students used the same teacher (110.1M parameter BERT-base models as both encoders), with the full Recall@5 = 72.3, Recall@20 = 86.1, and Recall@100 = 93.6.

Method	6-Layer (67.5M)			4-Layer (11.3M)		
	R@5	R@20	R@100	R@5	R@20	R@100
Train student directly	36.2	59.7	80.0	24.8	44.7	67.5
+ Distill from teacher	65.3	81.6	91.2	44.3	64.9	81.0
+ Inherit doc embeddings	69.9	83.9	92.3	56.3	70.9	82.5
+ Query embedding matching	72.7	86.5	93.9	61.2	75.2	85.1
+ Query generation	73.4	86.3	93.8	64.3	77.8	87.9
Train student using only embedding matching and inherit doc embeddings	71.4	84.9	92.6	64.6	50.2	76.8
+ Query generation	71.8	85.0	93.0	54.2	68.9	80.8

Next, we focus on the first term $\mathcal{E}_n(\mathcal{F}, \mathcal{G})$ which captures the uniform deviation between the training and test time performance of the student, as measured by the distillation loss. Again, we restrict ourselves to the setting of Theorem 5.1 which assumes a binary cross-entropy loss with $L = 1$ for simplicity. (See Appendix C.2 for a more precise statement and proof.)

Proposition 5.2. *Let ℓ_d be a distillation loss which is L_{ℓ_d} -Lipschitz in its first argument. Let \mathcal{F} and \mathcal{G} denote the function classes for the query and document encoders, respectively. Further assume that, for each query and document encoder in our function class, the query and document embeddings have their ℓ_2 -norm bounded by K . Then,*

$$\mathcal{E}_n(\mathcal{F}, \mathcal{G}) \leq \mathbb{E}_{\mathcal{I}_n} \frac{48KL_{\ell_d}}{\sqrt{n}} \int_0^\infty \sqrt{\log(N(u, \mathcal{F})N(u, \mathcal{G}))} du. \quad (6)$$

Furthermore, with a fixed document encoder, i.e., $\mathcal{G} = \{g^*\}$,

$$\mathcal{E}_n(\mathcal{F}, \{g^*\}) \leq \mathbb{E}_{\mathcal{I}_n} \frac{48KL_{\ell_d}}{\sqrt{n}} \int_0^\infty \sqrt{\log N(u, \mathcal{F})} du. \quad (7)$$

Here, $N(u, \cdot)$ is the u -covering number of a function class.

Note that Eq. 6 and Eq. 7 correspond to uniform deviation when we train *without* and *with* a frozen document encoder, respectively. It is clear that the bound in Eq. 7 is less than or equal to that in Eq. 6 (because $N(u, \mathcal{G}) \geq 1$ for any u), which alludes to desirable impact of employing a frozen document encoder (in terms of deviation in train and test performance). When we further employ EmbedDistill (e.g., with the loss in Eq. 5), it regularizes the function class of query encoders; effectively, reducing it to \mathcal{F}' with $|\mathcal{F}'| \leq |\mathcal{F}|$. This has further desirable implication for reducing the uniform deviation bounds as $N(u, \mathcal{F}') \leq N(u, \mathcal{F})$.

6 Experiments

We now conduct a comprehensive evaluation of the proposed distillation approach. Specifically, we highlight the utility of the approach for both DE to DE and CE to DE distillation. We also showcase the benefits of combining our distillation approach with query generation methods.

Table 2: Performance of EmbedDistill for DE to DE distillation on NQ test set. Note that the prior work mentioned in the table rely on techniques such as negative mining and multi-stage training. In contrast, we explore the orthogonal direction of embedding-matching that improves *single-stage* distillation, which can be combined with the aforementioned techniques.

Method	#Layers	R@20	R@100
DPR [Karpukhin et al., 2020a]	12	78.4	85.4
DPR + PAQ [Oğuz et al., 2021]	12	84.0	89.2
DPR + PAQ [Oğuz et al., 2021]	24	84.7	89.2
ACNE [Xiong et al., 2021]	12	81.9	87.5
RocketQA [Qu et al., 2021]	12	82.7	88.5
MSS-DPR [Sachan et al., 2021]	12	84.0	89.2
MSS-DPR [Sachan et al., 2021]	24	84.8	89.8
Our teacher [Zhang et al., 2022]	12 (220.2M)	85.4	90.0
Student w/ proposed method	6 (67.5M)	85.1	89.8
Student w/ proposed method	4 (11.3M)	81.2	87.4

6.1 Setup

Benchmarks and evaluation metrics. We consider two popular IR benchmarks — Natural Questions (NQ; Kwiatkowski et al. 2019b) and MSMARCO [Nguyen et al., 2016], which focus on finding the most relevant passage/document given a question and a search query, respectively. NQ provides both standard test and dev sets, whereas MSMARCO has only standard dev set publicly available. In what follows, we use the terms query (document) and question (passages) interchangeably. For NQ, we use the standard full recall (*strict*) as well as the *relaxed* recall metric [Karpukhin et al., 2020a] to evaluate the retrieval performance. For MSMARCO, we focus on the standard metrics *Mean Reciprocal Rank* (MRR)@10, and *normalized Discounted Cumulative Gain* (nDCG)@10 to evaluate both re-ranking and retrieval performance. See Appendix D for a detailed discussion on these evaluation metrics. Finally, we also evaluate EmbedDistill on the BEIR benchmark [Thakur et al., 2021] – a zero-shot retrieval benchmark – in terms of nDCG@10 and recall@100 metrics.

Model architectures. We follow the standard Transformers-based IR model architectures similar to Karpukhin et al. [2020a], Qu et al. [2021], Oğuz et al. [2021]. Our CE model is based on a RoBERTa-base model (Liu et al. [2019]; 12-layer, 768 dim, 124M parameters). We utilized various sizes of DE models based on BERT-base ([Devlin et al., 2019], 12-layer, 768 dim, 110M parameters), DistilBERT (Sanh et al. [2019]; 6-layer, 768 dim, 67.5M parameters – $\sim 2/3$ of base), or BERT-mini (Turc et al. [2019]; 4-layer, 256 dim, 11.3M parameters – $\sim 1/10$ of base). For query generation (cf. Sec. 4.3), we employ BART-base [Lewis et al., 2020], an encoder-decoder model, to generate similar questions from each training example’s input question (query). We randomly mask 10% of tokens and inject zero mean Gaussian noise with $\sigma = \{0.1, 0.2\}$ between the encoder and decoder. See Appendix E for more details on query generation and Appendix F.1 for hyperparameters.

Table 3: Performance of various DE models on MSMARCO dev set for *re-ranking* task. A teacher model (110.1M parameter BERT-base models as both encoders) achieving MRR@10 of 36.8 and nDCG@10 of 42.7 is used. The table shows performance of the symmetric DE student model (67.5M or 11.3M transformer as both encoders), and asymmetric DE student model (67.5M or 11.3M transformer as query encoder and document embeddings inherited from the teacher).

Method	MRR@10		nDCG@10	
	67.5M	11.3M	67.5M	11.3M
Train student directly	27.0	23.0	32.2	29.7
+ Distill from teacher	34.6	30.4	40.2	35.8
+ Inherit doc embeddings	35.2	32.1	41.0	37.7
+ Query embedding matching	36.2	35.0	42.0	40.8
+ Query generation	36.2	34.4	42.0	40.1
Train student using only embedding matching and inherit doc embeddings	36.5	33.5	42.3	39.3
+ Query generation	36.4	34.1	42.3	39.9

6.2 DE to DE distillation

We employ AR2 [Zhang et al., 2022]³ and SentenceBERT-v5 [Reimers et al., 2019]⁴ as teacher DE models for NQ and MSMARCO. Note that both models are based on BERT-base. For DE to DE distillation, we consider two kinds of configurations for the student DE model: (1) *Symmetric*: We use identical question and document encoders. We evaluate DistilBERT and BERT-mini on both datasets. (2) *Asymmetric*: The student DE model inherits its document embeddings from the teacher DE model, which *are not* trained during the distillation. For query encoder, we use DistilBERT or BERT-mini which are smaller than document encoder.

Student DE model training. We train student DE models using a combination of (i) one-hot loss (cf. Eq. 8 in Appendix A) on training data; (ii) distillation loss in (cf. Eq. 10 in Appendix A); and (iii) embedding matching loss in Eq. 5. We used [CLS]-pooling for all student encoders. Unlike DPR [Karpukhin et al., 2020a] or AR2, we do not use hard negatives from BM25 or other models, which greatly simplifies our distillation procedure.

Results and discussion. To understand the impact of various proposed configurations and losses, we train models by sequentially adding components and evaluate their retrieval performance on NQ and MSMARCO dev set as shown in Table 1 and 4, respectively. (See Table 7 in Appendix F.2 for performance on NQ in terms of the relaxed recall.) We also evaluate re-ranking task on MSMARCO dev set (Table 3).

We begin by training a symmetric DE without distillation. As expected, moving to distillation brings in considerable gains. Next, we swap the student document encoder with document embeddings from the teacher (non-trainable), which leads to a good jump in the performance. Now we can introduce EmbedDistill with Eq. 5 for aligning query representations between student and teacher. The two losses are combined with weight of 1.0 (except for BERT-mini models in the presence of query generation with 5.0). This improves performance significantly, e.g., it provides ~ 3 and ~ 5 points increase in recall@5 on NQ with students based on DistilBERT and BERT-mini, respectively (Table 1). We further explore the utility of EmbedDistill in aligning the teacher and student embedding spaces in Appendix G.1.

³<https://github.com/microsoft/AR2/tree/main/AR2>

⁴<https://huggingface.co/sentence-transformers/msmarco-bert-base-dot-v5>

Table 4: Performance of various DE models on MSMARCO dev set for *retrieval* task. A teacher model (110.1M parameter RoBERTa-base models as both encoders) achieving MRR@10 of 37.2 and nDCG@10 of 44.2 is used. The table shows performance of the symmetric DE student model (67.5M or 11.3M transformer as both encoders), and asymmetric DE student model (67.5M or 11.3M transformer as query encoder and document embeddings inherited from the teacher).

Method	MRR@10		nDCG@10	
	67.5M	11.3M	67.5M	11.3M
Train student directly	22.6	18.6	27.2	22.5
+ Distill from teacher	35.0	28.6	41.3	34.1
+ Inherit doc embeddings	35.7	30.3	42.2	36.2
+ Query embedding matching	37.1	35.4	43.8	41.9
+ Query generation	37.2	34.8	43.8	41.2
Train student using only embedding matching and inherit doc embeddings	36.6	31.4	43.3	37.6
+ Query generation	36.7	32.8	43.4	39.2

Table 5: Average BEIR performance of our DE teacher and EmbedDistill student models and their numbers of trainable parameters. Both models are trained on MSMARCO and evaluated on 14 other datasets (the average does not include MSMARCO). The full table is at Appendix F.4. With EmbedDistill, student materializes most of the performance of the teacher on the unforeseen datasets.

Method	#Layers	nDCG@10	R@100
DPR [Karpukhin et al., 2020b]	12	22.5	47.7
ANCE [Xiong et al., 2021]	12	40.5	60.0
TAS-B [Hofstätter et al., 2021]	6	42.8	64.8
GenQ [Thakur et al., 2021]	6	42.5	64.2
Our teacher [Reimers et al., 2019]	12 (220.2M)	45.7	65.1
Student w/ EmbedDistill	6 (67.5M)	44.0	63.5

On top of the two losses (standard distillation and embedding matching), we also use $R_{\text{Emb},Q}(t, s; \mathcal{Q}')$ from Sec. 4.3 on 2 additional questions (per input question) generated from BART. We also try a variant where we eliminate the standard distillation loss and only employ the embedding matching loss in Eq. 5 along with inheriting teacher’s document embeddings. This configuration without the standard distillation loss leads to excellent performance (with query generation again providing additional gains in most cases.)

It is worth highlighting that DE models trained with the proposed methods (e.g., asymmetric DE with embedding matching and generation) achieve 99% of the performance in both NQ/MSMARCO tasks with a query encoder that is 2/3rd the size of that of the teacher. Furthermore, even with 1/10th size of the query encoder, our proposal can achieve 95-97% of the performance. This is particularly useful for latency critical applications with minimal impact on the final performance.

Finally, we take our best student models, i.e., one trained using with additional embedding matching loss and using data augmentation from query generation, and evaluate on test sets. We compare with various prior work and note that most prior work used considerably bigger models in terms of parameters, depth (12 or 24 layers), or width (upto 1024 dims). For NQ test set results are reported in Table 2, but as MSMARCO does not have any public test set, we instead present results for the BEIR benchmark in Table 5. Note we

Table 6: Performance of DE models distilled from [CLS]-pooled and Dual-pooled CE models on MSMARCO re-ranking task. While both teacher models perform similarly, embedding matching-based distillation only works with the Dual-pooled teacher. See Appendix F for nDCG@10 metric.

Method	MRR@10
[CLS] -pooled teacher	37.1
Dual-pooled teacher	37.0
Standard distillation from [CLS]-pooled teacher	33.0
+Joint matching	32.4
Standard distillation from Dual-pooled teacher	33.3
+Query matching	33.7

also provide evaluation of our SentenceBERT teacher achieving very high performance on the benchmark which can be of independent interest (please refer to Appendix F.4 for details). For both NQ and BEIR, our approach obtains competitive student model with fewer than 50% of the parameters: even with 6 layers, our student model is very close (98-99%) to its teacher.

6.3 CE to DE distillation

We consider two CE teachers for MSMARCO re-ranking task⁵: a standard [CLS]-pooled CE teacher, and the Dual-pooled CE teacher (cf. Sec. 4.2). Both teachers are based on RoBERTa-base and trained on triples in the training set for 300K steps with cross-entropy loss.

Student DE model training. We considered the following distillation variants: standard score-based distillation from the [CLS]-pooled teacher, and our novel Dual-pooled CE teacher (with and without embedding matching loss). For each variant, we initialize encoders of the student DE model with two RoBERTa-base models and train for 500K steps. We performed the naïve joint embedding matching for the [CLS]-pooled teacher (cf. Sec. 4.2) and employed the query embedding matching (cf. Eq.5) for the Dual-pooled CE teacher. In either case, embedding-matching loss is added on top of the standard cross entropy loss with the weight of 1.0 (when used).

Results and discussion. Table 6 evaluates the effectiveness of the dual pooling and the embedding matching for CE to DE distillation. As described in Sec. 4.2, the traditional [CLS]-pooled teacher did not provide any useful embedding for the embedding matching (see Appendix G.2 for the further analysis of the resulting embedding space). However, with the Dual-pooled teacher, embedding matching does boost student’s performance.

7 Conclusion

We propose EmbedDistill — a novel distillation method for IR that goes beyond simple score matching. We specialize it to distill a DE model into another DE model by (a) reusing the teacher’s document encoder in the student and (b) aligning query embeddings of the teacher and student. This simple approach delivers immediate quality and computational gains in practical deployments and we demonstrate them on MSMARCO, NQ, and BEIR benchmarks. We show that query generation technique further improves the performance of the distilled student in most cases. We generalize the proposed approach to distill a CE model to a DE model

⁵Note: Full retrieval is prohibitively expensive with CE models.

and show the benefits on MSMARCO. Finally, our theoretical analysis alludes to the favorable implications of both embedding matching and inheriting document encoder in DE to DE distillation setting. A more comprehensive and systematic analysis of embedding matching-based distillation for IR is an exciting avenue for future research.

References

- Gustavo Aguilar, Yuan Ling, Yu Zhang, Benjamin Yao, Xing Fan, and Chenlei Guo. Knowledge distillation from internal representations. In *Proceedings of the AAAI Conference on Artificial Intelligence*, volume 34, pages 7350–7357, 2020.
- Chris Alberti, Daniel Andor, Emily Pitler, Jacob Devlin, and Michael Collins. Synthetic QA corpora generation with roundtrip consistency. In *Proceedings of the 57th Annual Meeting of the Association for Computational Linguistics*, pages 6168–6173, Florence, Italy, July 2019. Association for Computational Linguistics. doi: 10.18653/v1/P19-1620. URL <https://aclanthology.org/P19-1620>.
- Olivier Bousquet, Stéphane Boucheron, and Gábor Lugosi. *Introduction to Statistical Learning Theory*, pages 169–207. Springer Berlin Heidelberg, Berlin, Heidelberg, 2004. ISBN 978-3-540-28650-9. doi: 10.1007/978-3-540-28650-9_8. URL https://doi.org/10.1007/978-3-540-28650-9_8.
- Cristian Bucilă, Rich Caruana, and Alexandru Niculescu-Mizil. Model compression. In *Proceedings of the 12th ACM SIGKDD International Conference on Knowledge Discovery and Data Mining*, KDD ’06, pages 535–541, New York, NY, USA, 2006. ACM.
- Danqi Chen, Adam Fisch, Jason Weston, and Antoine Bordes. Reading Wikipedia to answer open-domain questions. In *Proceedings of the 55th Annual Meeting of the Association for Computational Linguistics (Volume 1: Long Papers)*, pages 1870–1879, Vancouver, Canada, July 2017. Association for Computational Linguistics. doi: 10.18653/v1/P17-1171. URL <https://aclanthology.org/P17-1171>.
- Defang Chen, Jian-Ping Mei, Hailin Zhang, Can Wang, Yan Feng, and Chun Chen. Knowledge distillation with the reused teacher classifier. In *Proceedings of the IEEE/CVF Conference on Computer Vision and Pattern Recognition*, pages 11933–11942, 2022.
- Xuanang Chen, Ben He, Kai Hui, Le Sun, and Yingfei Sun. Simplified tinybert: Knowledge distillation for document retrieval. In Djoerd Hiemstra, Marie-Francine Moens, Josiane Mothe, Raffaele Perego, Martin Potthast, and Fabrizio Sebastiani, editors, *Advances in Information Retrieval*, pages 241–248, Cham, 2021. Springer International Publishing. ISBN 978-3-030-72240-1.
- Zhuyun Dai and Jamie Callan. Deeper text understanding for IR with contextual neural language modeling. In Benjamin Piwowarski, Max Chevalier, Éric Gaussier, Yoelle Maarek, Jian-Yun Nie, and Falk Scholer, editors, *Proceedings of the 42nd International ACM SIGIR Conference on Research and Development in Information Retrieval, SIGIR 2019, Paris, France, July 21-25, 2019*, pages 985–988. ACM, 2019a.
- Zhuyun Dai and Jamie Callan. Context-aware sentence/passage term importance estimation for first stage retrieval. *arXiv preprint arXiv:1910.10687*, 2019b.
- Jacob Devlin, Ming-Wei Chang, Kenton Lee, and Kristina Toutanova. BERT: pre-training of deep bidirectional transformers for language understanding. In Jill Burstein, Christy Doran, and Thamar Solorio, editors, *Proceedings of the 2019 Conference of the North American Chapter of the Association for Computational Linguistics: Human Language Technologies, NAACL-HLT 2019, Minneapolis, MN, USA, June 2-7, 2019, Volume 1 (Long and Short Papers)*, pages 4171–4186. Association for Computational Linguistics, 2019.

Ruiqi Guo, Philip Sun, Erik Lindgren, Quan Geng, David Simcha, Felix Chern, and Sanjiv Kumar. Accelerating large-scale inference with anisotropic vector quantization. In *International Conference on Machine Learning*, 2020. URL <https://arxiv.org/abs/1908.10396>.

Geoffrey Hinton, Oriol Vinyals, and Jeff Dean. Distilling the knowledge in a neural network, 2015.

Sebastian Hofstätter, Sophia Althammer, Michael Schröder, Mete Sertkan, and Allan Hanbury. Improving efficient neural ranking models with cross-architecture knowledge distillation. *CoRR*, abs/2010.02666, 2020. URL <https://arxiv.org/abs/2010.02666>.

Sebastian Hofstätter, Sheng-Chieh Lin, Jheng-Hong Yang, Jimmy Lin, and Allan Hanbury. Efficiently teaching an effective dense retriever with balanced topic aware sampling. In *Proceedings of the 44th International ACM SIGIR Conference on Research and Development in Information Retrieval, SIGIR '21*, page 113–122, New York, NY, USA, 2021. Association for Computing Machinery. ISBN 9781450380379. doi: 10.1145/3404835.3462891. URL <https://doi.org/10.1145/3404835.3462891>.

Gautier Izacard and Edouard Grave. Distilling knowledge from reader to retriever for question answering. In *International Conference on Learning Representations*, 2021. URL <https://openreview.net/forum?id=NTEz-6wysdb>.

Gautier Izacard, Mathild Caron, Lucas Hosseini, Sebastian Riedel, Piotr Bojanowski, Armand Joulin, and Edouard Grave. Unsupervised dense information retrieval with contrastive learning. *arXiv preprint arXiv:2112.09118*, 2021.

Xiaoqi Jiao, Yichun Yin, Lifeng Shang, Xin Jiang, Xiao Chen, Linlin Li, Fang Wang, and Qun Liu. TinyBERT: Distilling BERT for natural language understanding. In *Findings of the Association for Computational Linguistics: EMNLP 2020*, pages 4163–4174, Online, November 2020. Association for Computational Linguistics. doi: 10.18653/v1/2020.findings-emnlp.372. URL <https://aclanthology.org/2020.findings-emnlp.372>.

Jeff Johnson, Matthijs Douze, and Hervé Jégou. Billion-scale similarity search with gpus. *IEEE Transactions on Big Data*, 7(3):535–547, 2021. doi: 10.1109/TBDA.2019.2921572.

Vladimir Karpukhin, Barlas Oğuz, Sewon Min, Patrick Lewis, Ledell Wu, Sergey Edunov, Danqi Chen, and Wen-tau Yih. Dense passage retrieval for open-domain question answering. In *Proceedings of the 2020 Conference on Empirical Methods in Natural Language Processing (EMNLP)*, pages 6769–6781, Online, November 2020a. Association for Computational Linguistics.

Vladimir Karpukhin, Barlas Oğuz, Sewon Min, Patrick Lewis, Ledell Wu, Sergey Edunov, Danqi Chen, and Wen-tau Yih. Dense passage retrieval for open-domain question answering. *arXiv preprint arXiv:2004.04906*, 2020b.

Omar Khattab and Matei Zaharia. *ColBERT: Efficient and Effective Passage Search via Contextualized Late Interaction over BERT*, page 39–48. Association for Computing Machinery, New York, NY, USA, 2020. ISBN 9781450380164.

Tom Kwiatkowski, Jennimaria Palomaki, Olivia Redfield, Michael Collins, Ankur Parikh, Chris Alberti, Danielle Epstein, Illia Polosukhin, Jacob Devlin, Kenton Lee, Kristina Toutanova, Llion Jones, Matthew Kelcey, Ming-Wei Chang, Andrew M. Dai, Jakob Uszkoreit, Quoc Le, and Slav Petrov. Natural questions: A benchmark for question answering research. *Transactions of the Association for Computational Linguistics*, 7:452–466, 2019a. doi: 10.1162/tacl_a_00276. URL <https://aclanthology.org/Q19-1026>.

Tom Kwiatkowski, Jennimaria Palomaki, Olivia Redfield, Michael Collins, Ankur Parikh, Chris Alberti, Danielle Epstein, Illia Polosukhin, Jacob Devlin, Kenton Lee, et al. Natural questions: a benchmark for question answering research. *Transactions of the Association for Computational Linguistics*, 7:453–466, 2019b.

Michel Ledoux and Michel Talagrand. *Probability in Banach spaces*. Springer-Verlag, 1991.

Kenton Lee, Ming-Wei Chang, and Kristina Toutanova. Latent retrieval for weakly supervised open domain question answering. In Anna Korhonen, David R. Traum, and Lluís Màrquez, editors, *Proceedings of the 57th Conference of the Association for Computational Linguistics, ACL 2019, Florence, Italy, July 28–August 2, 2019, Volume 1: Long Papers*, pages 6086–6096. Association for Computational Linguistics, 2019.

Mike Lewis, Yinhan Liu, Naman Goyal, Marjan Ghazvininejad, Abdelrahman Mohamed, Omer Levy, Veselin Stoyanov, and Luke Zettlemoyer. BART: Denoising sequence-to-sequence pre-training for natural language generation, translation, and comprehension. In *Proceedings of the 58th Annual Meeting of the Association for Computational Linguistics*, pages 7871–7880, Online, July 2020. Association for Computational Linguistics. doi: 10.18653/v1/2020.acl-main.703. URL <https://aclanthology.org/2020.acl-main.703>.

Canjia Li, Andrew Yates, Sean MacAvaney, Ben He, and Yingfei Sun. Parade: Passage representation aggregation for document reranking. *arXiv preprint arXiv:2008.09093*, 2020.

Sheng-Chieh Lin, Jheng-Hong Yang, and Jimmy Lin. In-batch negatives for knowledge distillation with tightly-coupled teachers for dense retrieval. In *Proceedings of the 6th Workshop on Representation Learning for NLP (RepL4NLP-2021)*, pages 163–173, Online, August 2021. Association for Computational Linguistics. doi: 10.18653/v1/2021.repl4nlp-1.17. URL <https://aclanthology.org/2021.repl4nlp-1.17>.

Yinhan Liu, Myle Ott, Naman Goyal, Jingfei Du, Mandar Joshi, Danqi Chen, Omer Levy, Mike Lewis, Luke Zettlemoyer, and Veselin Stoyanov. Roberta: A robustly optimized bert pretraining approach. *arXiv preprint arXiv:1907.11692*, 2019.

Wenhuo Lu, Jian Jiao, and Ruofei Zhang. Twinbert: Distilling knowledge to twin-structured compressed bert models for large-scale retrieval. In *Proceedings of the 29th ACM International Conference on Information & Knowledge Management, CIKM '20*, page 2645–2652, New York, NY, USA, 2020. Association for Computing Machinery. ISBN 9781450368599. doi: 10.1145/3340531.3412747. URL <https://doi.org/10.1145/3340531.3412747>.

Yi Luan, Jacob Eisenstein, Kristina Toutanova, and Michael Collins. Sparse, dense, and attentional representations for text retrieval. *Transactions of the Association for Computational Linguistics*, 9:329–345, 2021. doi: 10.1162/tacl_a_00369. URL <https://aclanthology.org/2021.tacl-1.20>.

Ji Ma, Ivan Korotkov, Yinfei Yang, Keith Hall, and Ryan McDonald. Zero-shot neural passage retrieval via domain-targeted synthetic question generation. In *Proceedings of the 16th Conference of the European Chapter of the Association for Computational Linguistics: Main Volume*, pages 1075–1088, Online, April 2021. Association for Computational Linguistics. doi: 10.18653/v1/2021.eacl-main.92. URL <https://aclanthology.org/2021.eacl-main.92>.

Sean MacAvaney, Andrew Yates, Arman Cohan, and Nazli Goharian. CEDR: Contextualized embeddings for document ranking. In *Proceedings of the 42nd International ACM SIGIR Conference on Research*

and Development in Information Retrieval, SIGIR’19, page 1101–1104, New York, NY, USA, 2019a. Association for Computing Machinery. ISBN 9781450361729. doi: 10.1145/3331184.3331317. URL <https://doi.org/10.1145/3331184.3331317>.

Sean MacAvaney, Andrew Yates, Kai Hui, and Ophir Frieder. Content-based weak supervision for ad-hoc re-ranking. In *Proceedings of the 42nd International ACM SIGIR Conference on Research and Development in Information Retrieval, SIGIR’19*, page 993–996, New York, NY, USA, 2019b. Association for Computing Machinery. ISBN 9781450361729. doi: 10.1145/3331184.3331316. URL <https://doi.org/10.1145/3331184.3331316>.

Sean MacAvaney, Franco Maria Nardini, Raffaele Perego, Nicola Tonelotto, Nazli Goharian, and Ophir Frieder. *Efficient Document Re-Ranking for Transformers by Precomputing Term Representations*, page 49–58. Association for Computing Machinery, New York, NY, USA, 2020. ISBN 9781450380164.

Aditya Menon, Sadeep Jayasumana, Ankit Singh Rawat, Seungyeon Kim, Sashank Reddi, and Sanjiv Kumar. In defense of dual-encoders for neural ranking. In Kamalika Chaudhuri, Stefanie Jegelka, Le Song, Csaba Szepesvari, Gang Niu, and Sivan Sabato, editors, *Proceedings of the 39th International Conference on Machine Learning*, volume 162 of *Proceedings of Machine Learning Research*, pages 15376–15400. PMLR, 17–23 Jul 2022. URL <https://proceedings.mlr.press/v162/menon22a.html>.

Bhaskar Mitra and Nick Craswell. An introduction to neural information retrieval. *Foundations and Trends® in Information Retrieval*, 13(1):1–126, 2018. ISSN 1554-0669. doi: 10.1561/1500000061. URL <http://dx.doi.org/10.1561/1500000061>.

Tri Nguyen, Mir Rosenberg, Xia Song, Jianfeng Gao, Saurabh Tiwary, Rangan Majumder, and Li Deng. MS MARCO: A human generated machine reading comprehension dataset. In Tarek Richard Besold, Antoine Bordes, Artur S. d’Avila Garcez, and Greg Wayne, editors, *Proceedings of the Workshop on Cognitive Computation: Integrating neural and symbolic approaches 2016*, volume 1773 of *CEUR Workshop Proceedings*. CEUR-WS.org, 2016.

Ping Nie, Yuyu Zhang, Xiubo Geng, Arun Ramamurthy, Le Song, and Dixin Jiang. DC-BERT: decoupling question and document for efficient contextual encoding. In Jimmy Huang, Yi Chang, Xueqi Cheng, Jaap Kamps, Vanessa Murdock, Ji-Rong Wen, and Yiqun Liu, editors, *Proceedings of the 43rd International ACM SIGIR conference on research and development in Information Retrieval, SIGIR 2020, Virtual Event, China, July 25-30, 2020*, pages 1829–1832. ACM, 2020. doi: 10.1145/3397271.3401271. URL <https://doi.org/10.1145/3397271.3401271>.

Rodrigo Nogueira and Kyunghyun Cho. Passage re-ranking with BERT. *CoRR*, abs/1901.04085, 2019. URL <http://arxiv.org/abs/1901.04085>.

Rodrigo Nogueira, Jimmy Lin, and AI Epistemic. From doc2query to docttttquery. *Online preprint*, 6, 2019a.

Rodrigo Nogueira, Wei Yang, Jimmy Lin, and Kyunghyun Cho. Document expansion by query prediction. *arXiv preprint arXiv:1904.08375*, 2019b.

Rodrigo Nogueira, Zhiying Jiang, Ronak Pradeep, and Jimmy Lin. Document ranking with a pretrained sequence-to-sequence model. In *Findings of the Association for Computational Linguistics: EMNLP 2020*, pages 708–718, Online, November 2020. Association for Computational Linguistics. doi: 10.18653/v1/2020.findings-emnlp.63. URL <https://aclanthology.org/2020.findings-emnlp.63>.

Barlas Oğuz, Kushal Lakhotia, Anchit Gupta, Patrick Lewis, Vladimir Karpukhin, Aleksandra Piktus, Xilun Chen, Sebastian Riedel, Wen-tau Yih, Sonal Gupta, et al. Domain-matched pre-training tasks for dense retrieval. *arXiv preprint arXiv:2107.13602*, 2021.

Yingqi Qu, Yuchen Ding, Jing Liu, Kai Liu, Ruiyang Ren, Wayne Xin Zhao, Daxiang Dong, Hua Wu, and Haifeng Wang. RocketQA: An optimized training approach to dense passage retrieval for open-domain question answering. In Kristina Toutanova, Anna Rumshisky, Luke Zettlemoyer, Dilek Hakkani-Tür, Iz Beltagy, Steven Bethard, Ryan Cotterell, Tanmoy Chakraborty, and Yichao Zhou, editors, *Proceedings of the 2021 Conference of the North American Chapter of the Association for Computational Linguistics: Human Language Technologies, NAACL-HLT 2021, Online, June 6-11, 2021*, pages 5835–5847. Association for Computational Linguistics, 2021.

Colin Raffel, Noam Shazeer, Adam Roberts, Katherine Lee, Sharan Narang, Michael Matena, Yanqi Zhou, Wei Li, and Peter J. Liu. Exploring the limits of transfer learning with a unified text-to-text transformer. *Journal of Machine Learning Research*, 21(140):1–67, 2020. URL <http://jmlr.org/papers/v21/20-074.html>.

Nils Reimers, Iryna Gurevych, and Iryna Gurevych. Sentence-BERT: Sentence embeddings using siamese bert-networks. In *Proceedings of the 2019 Conference on Empirical Methods in Natural Language Processing*. Association for Computational Linguistics, 11 2019. URL <http://arxiv.org/abs/1908.10084>.

Ruiyang Ren, Yingqi Qu, Jing Liu, Wayne Xin Zhao, Qiaoqiao She, Hua Wu, Haifeng Wang, and Ji-Rong Wen. Rocketqav2: A joint training method for dense passage retrieval and passage re-ranking. In *Proceedings of EMNLP*, 2021.

Adriana Romero, Nicolas Ballas, Samira Ebrahimi Kahou, Antoine Chassang, Carlo Gatta, and Yoshua Bengio. Fitnets: Hints for thin deep nets. *arXiv preprint arXiv:1412.6550*, 2014.

Devendra Sachan, Mostofa Patwary, Mohammad Shoeybi, Neel Kant, Wei Ping, William L. Hamilton, and Bryan Catanzaro. End-to-end training of neural retrievers for open-domain question answering. In *Proceedings of the 59th Annual Meeting of the Association for Computational Linguistics and the 11th International Joint Conference on Natural Language Processing (Volume 1: Long Papers)*, pages 6648–6662, Online, August 2021. Association for Computational Linguistics. doi: 10.18653/v1/2021.acl-long.519. URL <https://aclanthology.org/2021.acl-long.519>.

Devendra Singh Sachan, Mike Lewis, Mandar Joshi, Armen Aghajanyan, Wen-tau Yih, Joelle Pineau, and Luke Zettlemoyer. Improving passage retrieval with zero-shot question generation. *arXiv preprint arXiv:2204.07496*, 2022.

Victor Sanh, Lysandre Debut, Julien Chaumond, and Thomas Wolf. Distilbert, a distilled version of bert: smaller, faster, cheaper and lighter. *arXiv preprint arXiv:1910.01108*, 2019.

Keshav Santhanam, Omar Khattab, Jon Saad-Falcon, Christopher Potts, and Matei Zaharia. Colbertv2: Effective and efficient retrieval via lightweight late interaction. *CoRR*, abs/2112.01488, 2021.

Nandan Thakur, Nils Reimers, Andreas Rücklé, Abhishek Srivastava, and Iryna Gurevych. BEIR: A heterogeneous benchmark for zero-shot evaluation of information retrieval models. In *Thirty-fifth Conference on Neural Information Processing Systems Datasets and Benchmarks Track (Round 2)*, 2021. URL <https://openreview.net/forum?id=wCu6T5xFjeJ>.

Iulia Turc, Ming-Wei Chang, Kenton Lee, and Kristina Toutanova. Well-read students learn better: On the importance of pre-training compact models. *arXiv preprint arXiv:1908.08962*, 2019.

Ashish Vaswani, Noam Shazeer, Niki Parmar, Jakob Uszkoreit, Llion Jones, Aidan N. Gomez, Łukasz Kaiser, and Illia Polosukhin. Attention is all you need. In *Proceedings of the 31st International Conference on Neural Information Processing Systems*, NIPS’17, page 6000–6010, Red Hook, NY, USA, 2017. Curran Associates Inc. ISBN 9781510860964.

Lee Xiong, Chenyan Xiong, Ye Li, Kwok-Fung Tang, Jialin Liu, Paul N. Bennett, Junaid Ahmed, and Arnold Overwijk. Approximate nearest neighbor negative contrastive learning for dense text retrieval. In *International Conference on Learning Representations*, 2021. URL <https://openreview.net/forum?id=zeFrfgyzln>.

Zeynep Akkalyoncu Yilmaz, Wei Yang, Haotian Zhang, and Jimmy Lin. Cross-domain modeling of sentence-level evidence for document retrieval. In *Proceedings of the 2019 Conference on Empirical Methods in Natural Language Processing and the 9th International Joint Conference on Natural Language Processing (EMNLP-IJCNLP)*, pages 3490–3496, Hong Kong, China, November 2019. Association for Computational Linguistics.

Hang Zhang, Yeyun Gong, Yelong Shen, Jiancheng Lv, Nan Duan, and Weizhu Chen. Adversarial retriever-ranker for dense text retrieval. In *International Conference on Learning Representations*, 2022. URL <https://openreview.net/forum?id=MR7XubKUFB>.

Linfeng Zhang and Kaisheng Ma. Improve object detection with feature-based knowledge distillation: Towards accurate and efficient detectors. In *International Conference on Learning Representations*, 2020.

Shuai Zhang, Lina Yao, Aixin Sun, and Yi Tay. Deep learning based recommender system: A survey and new perspectives. *ACM Comput. Surv.*, 52(1), feb 2019. ISSN 0360-0300. doi: 10.1145/3285029. URL <https://doi.org/10.1145/3285029>.

Chen Zhao, Chenyan Xiong, Jordan Boyd-Graber, and Hal Daumé III. Distantly-supervised dense retrieval enables open-domain question answering without evidence annotation. In *Proceedings of the 2021 Conference on Empirical Methods in Natural Language Processing*, pages 9612–9622, Online and Punta Cana, Dominican Republic, November 2021. Association for Computational Linguistics. doi: 10.18653/v1/2021.emnlp-main.756. URL <https://aclanthology.org/2021.emnlp-main.756>.

Zhi Zheng, Kai Hui, Ben He, Xianpei Han, Le Sun, and Andrew Yates. BERT-QE: Contextualized Query Expansion for Document Re-ranking. In *Findings of the Association for Computational Linguistics: EMNLP 2020*, pages 4718–4728, Online, November 2020. Association for Computational Linguistics. doi: 10.18653/v1/2020.findings-emnlp.424. URL <https://aclanthology.org/2020.findings-emnlp.424>.

A Loss functions

Here, we state various (per-example) loss functions that most commonly define training objectives for IR models. Typically, one hot training with original label is performed using *softmax-based cross-entropy loss* functions:

$$\ell(s_{q,\mathbf{d}_i}, \mathbf{y}_i) = - \sum_{j \in [L]} y_{i,j} \cdot \log \left(\frac{\exp(s(q_i, d_{i,j}))}{\sum_{j' \in [L]} \exp(s(q_i, d_{i,j'}))} \right). \quad (8)$$

In our experiments, we use in-batch negatives for obtaining the irrelevant documents $d_{i,j'}$. Alternatively, it is also common to employ a one-vs-all loss function based on *binary cross-entropy loss* as follows:

$$\ell(s_{q,\mathbf{d}_i}, \mathbf{y}_i) = - \sum_{j \in [L]} \left(y_{i,j} \cdot \log \left(\frac{1}{1 + \exp(-s(q_i, d_{i,j}))} \right) + (1 - y_{i,j}) \cdot \log \left(\frac{1}{1 + \exp(s(q_i, d_{i,j}))} \right) \right). \quad (9)$$

As for distillation, one can define a distillation objective based on the softmax-based cross-entropy loss as⁶:

$$\ell_d(s_{q,\mathbf{d}_i}^s, s_{q,\mathbf{d}_i}^t) = - \sum_{j \in [L]} \left(\frac{\exp(s_{i,j}^t)}{\sum_{j' \in [L]} \exp(s_{i,j'}^t)} \cdot \log \left(\frac{\exp(s_{i,j}^s)}{\sum_{j' \in [L]} \exp(s_{i,j'}^s)} \right) \right), \quad (10)$$

where $s_{i,j}^t := s^t(q_i, d_{i,j})$ and $s_{i,j}^s := s^s(q_i, d_{i,j})$ denote the teacher and student scores, respectively. On the other hand, the distillation objective with the binary cross-entropy takes the form:

$$\ell_d(s_{q,\mathbf{d}_i}^s, s_{q,\mathbf{d}_i}^t) = - \sum_{j \in [L]} \left(\frac{1}{1 + \exp(-s_{i,j}^t)} \cdot \log \left(\frac{1}{1 + \exp(-s_{i,j}^s)} \right) + \frac{1}{1 + \exp(s_{i,j}^t)} \cdot \log \left(\frac{1}{1 + \exp(s_{i,j}^s)} \right) \right). \quad (11)$$

Finally, distillation based on the mean square error (MSE) loss (aka. logit matching) employs the following loss function:

$$\ell_d(s_{q,\mathbf{d}_i}^s, s_{q,\mathbf{d}_i}^t) = \sum_{j \in [L]} (s^t(q_i, d_{i,j}) - s^s(q_i, d_{i,j}))^2. \quad (12)$$

B Dual pooling details

In this work, we focus on two kinds of dual pooling strategies:

- **Special tokens-based dual pooling.** Let pool_{CLS} and pool_{SEP} denote the pooling operations that return the embeddings of the `[CLS]` and `[SEP]` tokens, respectively. We define

$$\begin{aligned} \text{emb}_{q \leftarrow (q,d)}^t &= \text{pool}_{\text{CLS}}(\text{Enc}^t(\tilde{o})), \\ \text{emb}_{d \leftarrow (q,d)}^t &= \text{pool}_{\text{SEP}}(\text{Enc}^t(\tilde{o})), \end{aligned} \quad (13)$$

where \tilde{o} denotes the input token sequence to the Transformers-based encoder, which consists of { query, document, special } tokens.

⁶It is common to employ temperature scaling with softmax operation. We do not explicitly show the temperature parameter for ease of exposition.

- **Segment-based weighted-mean dual pooling.** Let $\text{Enc}^t(\tilde{o})|_Q$ and $\text{Enc}^t(\tilde{o})|_D$ denote the final query token embeddings and document token embeddings produced by the encoder, respectively. We define the *proxy* query and document embeddings

$$\begin{aligned}\mathbf{emb}_{q \leftarrow (q, d)}^t &= \text{mean}_{\text{wt}}(\text{Enc}^t(\tilde{o})|_Q), \\ \mathbf{emb}_{d \leftarrow (q, d)}^t &= \text{mean}_{\text{wt}}(\text{Enc}^t(\tilde{o})|_D),\end{aligned}\tag{14}$$

where $\text{mean}_{\text{wt}}(\cdot)$ denotes the weighted mean operation. We employ the specific weighting scheme where each token receives a weight equal to the inverse of the square root of the token-sequence length.

C Deferred details and proofs from Section 5

In this section we present more precise statements and proofs of Theorem 5.1 and Proposition 5.2 (stated informally in Section 5 of the main text) along with the necessary background. First, for the ease of exposition, we define new notation which will facilitate theoretical analysis in this section.

Notation. Denote the query and document encoders as $f: \mathcal{Q} \rightarrow \mathbb{R}^k$ and $g: \mathcal{D} \rightarrow \mathbb{R}^k$ for the student, and $F: \mathcal{Q} \rightarrow \mathbb{R}^k, G: \mathcal{D} \rightarrow \mathbb{R}^k$ for the teacher (in the dual-encoder setting). With q denoting a query and d denoting a document, $f(q)$ and $g(d)$ then denote query and document embeddings, respectively, generated by the student. We define $F(q)$ and $G(d)$ similarly for embeddings by the teacher.⁷

Theorem C.1 (Formal statement of Theorem 5.1). *Let \mathcal{F} and \mathcal{G} denote the function classes for the query and document encoders for the student model, respectively. Given n examples $\mathcal{S}_n = \{(q_i, d_i, y_i)\}_{i \in [n]} \subset \mathcal{Q} \times \mathcal{D} \times \{0, 1\}$, let $s^s(q, d) := s^{f,g}(q_i, d_i) = f(q_i)^T g(d_i)$ be the scores assigned to the (q_i, d_i) pair by a dual-encoder model with $f \in \mathcal{F}$ and $g \in \mathcal{G}$ as query and document encoders, respectively. Let ℓ and ℓ_d be the binary cross-entropy loss (cf. Eq. 9 with $L = 1$) and the distillation-specific loss based on it (cf. Eq. 11 with $L = 1$), respectively. In particular,*

$$\begin{aligned}\ell(s^{F,G}(q_i, d_i), y_i) &:= -y_i \log \sigma(F(q_i)^T G(d_i)) - (1 - y_i) \log [1 - \sigma(F(q_i)^T G(d_i))] \\ \ell_d(s^{f,g}(q_i, d_i), s^{F,G}(q_i, d_i)) &:= -\sigma(F(q_i)^T G(d_i)) \cdot \log \sigma(f(q_i)^T g(d_i)) - \\ &\quad [1 - \sigma(F(q_i)^T G(d_i))] \cdot \log [1 - \sigma(f(q_i)^T g(d_i))],\end{aligned}$$

where σ is the sigmoid function and $s^t := s^{F,G}$ denotes the teacher dual-encoder model with F and G as its query and document encoders, respectively. Assume that

1. All encoders f, g, F , and G have the same output dimension.

2. $\exists K \in (0, \infty)$ such that

$$\sup_{q \in \mathcal{Q}} \max \{\|f(q)\|_2, \|F(q)\|_2\} \leq K$$

and

$$\sup_{d \in \mathcal{D}} \max \{\|g(d)\|_2, \|G(d)\|_2\} \leq K.$$

⁷Note that, as per the notations in the main text, we have $(f, g) = (\text{Enc}_Q^s, \text{Enc}_D^s)$ and $(F, G) = (\text{Enc}_Q^t, \text{Enc}_D^t)$. Similarly, we have $(\mathbf{emb}_q^t, \mathbf{emb}_d^t) = (f(q), g(d))$ and $(\mathbf{emb}_q^t, \mathbf{emb}_d^t) = (F(q), G(d))$.

Then, we have

$$\begin{aligned}
& \underbrace{\mathbb{E} [s^{f,g}(q, d)]}_{:=R(s^s)=R(s^{f,g})} - \underbrace{\mathbb{E} [s^{F,G}(q, d)]}_{:=R(s^t)=R(s^{F,G})} \leq \underbrace{\sup_{(f,g) \in \mathcal{F} \times \mathcal{G}} \left| R(s^{f,g}, s^{F,G}; \mathcal{S}_n) - \mathbb{E} [\ell_d(s^{f,g}(q, d), s^{F,G}(q, d))] \right|}_{:=\mathcal{E}_n(\mathcal{F}, \mathcal{G})} \\
& + 2K \left(\underbrace{\frac{1}{n} \sum_{i \in [n]} \|g(d_i) - G(d_i)\|_2}_{:=R_{\text{Emb}, D}(t, s; \mathcal{S}_n)} + \underbrace{\frac{1}{n} \sum_{i \in [n]} \|f(q_i) - F(q_i)\|_2}_{:=R_{\text{Emb}, Q}(t, s; \mathcal{S}_n)} \right) + \underbrace{R(s^{F,G}; \mathcal{S}_n) - R(s^{F,G})}_{:=\Delta(s^t; \mathcal{S}_n)} \\
& + K^2 \left(\mathbb{E} \left[\left| \sigma(F(q)^\top G(d)) - y \right| \right] + \frac{1}{n} \sum_{i \in [n]} \left| \sigma(F(q_i)^\top G(d_i)) - y_i \right| \right). \tag{15}
\end{aligned}$$

Proof. Note that

$$\begin{aligned}
R(s^{f,g}) - R(s^{F,G}) &= R(s^{f,g}) - R(s^{f,g}, s^{F,G}) + R(s^{f,g}, s^{F,G}) - R(s^{F,G}) \\
&\stackrel{(a)}{\leq} K^2 \mathbb{E} \left[\left| \sigma(F(q)^\top G(d)) - y \right| \right] + R(s^{f,g}, s^{F,G}) - R(s^{F,G}) \\
&= K^2 \mathbb{E} \left[\left| \sigma(F(q)^\top G(d)) - y \right| \right] + R(s^{f,g}, s^{F,G}) - R(s^{f,g}, s^{F,G}; \mathcal{S}_n) + R(s^{f,g}, s^{F,G}; \mathcal{S}_n) - R(s^{F,G}) \\
&\stackrel{(b)}{\leq} K^2 \mathbb{E} \left[\left| \sigma(F(q)^\top G(d)) - y \right| \right] + \mathcal{E}_n(\mathcal{F}, \mathcal{G}) + R(s^{f,g}, s^{F,G}; \mathcal{S}_n) - R(s^{F,G}) \\
&= K^2 \mathbb{E} \left[\left| \sigma(F(q)^\top G(d)) - y \right| \right] + \mathcal{E}_n(\mathcal{F}, \mathcal{G}) + R(s^{f,g}, s^{F,G}; \mathcal{S}_n) - R(s^{F,G}; \mathcal{S}_n) + \\
&\quad R(s^{F,G}; \mathcal{S}_n) - R(s^{F,G}) \\
&\stackrel{(c)}{\leq} K^2 \mathbb{E} \left[\left| \sigma(F(q)^\top G(d)) - y \right| \right] + \mathcal{E}_n(\mathcal{F}, \mathcal{G}) + \underbrace{R(s^{F,G}; \mathcal{S}_n) - R(s^{F,G})}_{:=\Delta(s^t; \mathcal{S}_n)} + \\
&\quad \frac{2K}{n} \sum_{i \in [n]} \|g(d_i) - G(d_i)\|_2 + \frac{2K}{n} \sum_{i \in [n]} \|f(q_i) - F(q_i)\|_2 + \frac{K^2}{n} \sum_{i \in [n]} \left| \sigma(F(q_i)^\top G(d_i)) - y_i \right| \tag{16}
\end{aligned}$$

where (a) follows from Lemma C.3, (b) follows from the definition of $\mathcal{E}_n(\mathcal{F}, \mathcal{G})$, and (c) follows from Proposition C.2. \square

C.1 Bounding the difference between student's empirical *distillation* risk and teacher's empirical risk

Lemma C.2. *Given n examples $\mathcal{S}_n = \{(q_i, d_i, y_i)\}_{i \in [n]} \subset \mathcal{Q} \times \mathcal{D} \times \{0, 1\}$, let $s^{f,g}(q_i, d_i) = f(q_i)^\top g(d_i)$ be the scores assigned to the (q_i, d_i) pair by a dual-encoder model with f and g as query and document encoders, respectively. Let ℓ and ℓ_d be the binary cross-entropy loss (cf. Eq. 9 with $L = 1$) and the distillation-specific loss based on it (cf. Eq. 11 with $L = 1$), respectively. In particular,*

$$\begin{aligned}
\ell(s^{F,G}(q_i, d_i), y_i) &:= -y_i \log \sigma(F(q_i)^\top G(d_i)) - (1 - y_i) \log [1 - \sigma(F(q_i)^\top G(d_i))] \\
\ell_d(s^{f,g}(q_i, d_i), s^{F,G}(q_i, d_i)) &:= -\sigma(F(q_i)^\top G(d_i)) \cdot \log \sigma(f(q_i)^\top g(d_i)) - \\
&\quad [1 - \sigma(F(q_i)^\top G(d_i))] \cdot \log [1 - \sigma(f(q_i)^\top g(d_i))],
\end{aligned}$$

where σ is the sigmoid function and $s^{F,G}$ denotes the teacher dual-encoder model with F and G as its query and document encoders, respectively. Assume that

1. All encoders f, g, F , and G have the same output dimension $k \geq 1$.
2. $\exists K \in (0, \infty)$ such that

$$\sup_{q \in \mathcal{Q}} \max \{ \|f(q)\|_2, \|F(q)\|_2 \} \leq K$$

and

$$\sup_{d \in \mathcal{D}} \max \{ \|g(d)\|_2, \|G(d)\|_2 \} \leq K.$$

Then, we have

$$\begin{aligned} & \frac{1}{n} \sum_{i \in [n]} \ell_d(s^{f,g}(q_i, d_i), s^{F,G}(q_i, d_i)) - \frac{1}{n} \sum_{i \in [n]} \ell(s^{F,G}(q_i, d_i), y_i) \leq \\ & \frac{2K}{n} \sum_{i \in [n]} \|g(d_i) - G(d_i)\|_2 + \frac{2K}{n} \sum_{i \in [n]} \|f(q_i) - F(q_i)\|_2 + \frac{K^2}{n} \sum_{i \in [n]} \left| \sigma(F(q_i)^\top G(d_i)) - y_i \right|. \end{aligned} \quad (17)$$

Proof. We first note that the distillation loss can be rewritten as

$$\ell_d(s^{f,g}(q, d), s^{F,G}(q, d)) = (1 - \sigma(F(q)^\top G(d))) f(q)^\top g(d) + \gamma(-f(q)^\top g(d)),$$

where $\gamma(v) := \log[1 + e^v]$ is the softplus function. Similarly, the one-hot (label-dependent) loss can be rewritten as

$$\ell(s^{F,G}(q, d), y) = (1 - y) F(q)^\top G(d) + \gamma(-F(q)^\top G(d)).$$

Recall from our notation in Section 3 that

$$R(s^{f,g}, s^{F,G}; \mathcal{S}_n) := \frac{1}{n} \sum_{i \in [n]} \ell_d(s^{f,g}(q_i, d_i), s^{F,G}(q_i, d_i)), \quad (18)$$

$$R(s^{F,G}; \mathcal{S}_n) := \frac{1}{n} \sum_{i \in [n]} \ell(s^{F,G}(q_i, d_i), y_i), \quad (19)$$

as the empirical risk based on the distillation loss, and the empirical risk based on the label-dependent loss, respectively. With this notation, the quantity to upper bound can be rewritten as

$$\begin{aligned} R(s^{f,g}, s^{F,G}; \mathcal{S}_n) - R(s^{F,G}; \mathcal{S}_n) &= \underbrace{R(s^{f,g}, s^{F,G}; \mathcal{S}_n) - R(s^{f,G}, s^{F,G}; \mathcal{S}_n)}_{:= \square_1} + \\ &\quad \underbrace{R(s^{f,G}, s^{F,G}; \mathcal{S}_n) - R(s^{F,G}, s^{F,G}; \mathcal{S}_n)}_{:= \square_2} + \\ &\quad \underbrace{R(s^{F,G}, s^{F,G}; \mathcal{S}_n) - R(s^{F,G}; \mathcal{S}_n)}_{:= \square_3}. \end{aligned} \quad (20)$$

We start by bounding \square_1 as

$$\square_1 = \frac{1}{n} \sum_{i \in [n]} \left(\ell_d(s^{f,g}(q_i, d_i), s^{F,G}(q_i, d_i)) - \ell_d(s^{f,G}(q_i, d_i), s^{F,G}(q_i, d_i)) \right)$$

$$\begin{aligned}
&= \frac{1}{n} \sum_{i \in [n]} \left(\left(1 - \sigma(F(q_i)^\top G(d_i)) \right) f(q_i)^\top g(d_i) + \gamma(-f(q_i)^\top g(d_i)) \right. \\
&\quad \left. - \left(1 - \sigma(F(q_i)^\top G(d_i)) \right) f(q_i)^\top G(d_i) - \gamma(-f(q_i)^\top G(d_i)) \right) \\
&= \frac{1}{n} \sum_{i \in [n]} \left(f(q_i)^\top (g(d_i) - G(d_i)) \left(1 - \sigma(F(q_i)^\top G(d_i)) \right) + \gamma(-f(q_i)^\top g(d_i)) - \gamma(-f(q_i)^\top G(d_i)) \right) \\
&\stackrel{(a)}{\leq} \frac{1}{n} \sum_{i \in [n]} \left(f(q_i)^\top (g(d_i) - G(d_i)) \left(1 - \sigma(F(q_i)^\top G(d_i)) \right) + \left| f(q_i)^\top g(d_i) - f(q_i)^\top G(d_i) \right| \right) \\
&\stackrel{(b)}{\leq} \frac{1}{n} \sum_{i \in [n]} \left(\|f(q_i)\| \|g(d_i) - G(d_i)\| \left(1 - \sigma(F(q_i)^\top G(d_i)) \right) + \|f(q_i)\| \|g(d_i) - G(d_i)\| \right) \\
&\leq \frac{K}{n} \sum_{i \in [n]} \|g(d_i) - G(d_i)\|_2 \left(2 - \sigma(F(q_i)^\top G(d_i)) \right) \\
&\leq \frac{2K}{n} \sum_{i \in [n]} \|g(d_i) - G(d_i)\|_2,
\end{aligned} \tag{21}$$

where at (a) we use the fact that γ is a Lipschitz continuous function with Lipschitz constant 1, and at (b) we use Cauchy-Schwarz inequality.

Similarly for \square_2 , we proceed as

$$\begin{aligned}
\square_2 &= \frac{1}{n} \sum_{i \in [n]} \left(\ell_d(s^{f,G}(q_i, d_i), s^{F,G}(q_i, d_i)) - \ell_d(s^{F,G}(q_i, d_i), s^{F,G}(q_i, d_i)) \right) \\
&= \frac{1}{n} \sum_{i \in [n]} \left(\left(1 - \sigma(F(q_i)^\top G(d_i)) \right) f(q_i)^\top G(d_i) + \gamma(-f(q_i)^\top G(d_i)) \right. \\
&\quad \left. - \left(1 - \sigma(F(q_i)^\top G(d_i)) \right) F(q_i)^\top G(d_i) - \gamma(-F(q_i)^\top G(d_i)) \right) \\
&= \frac{1}{n} \sum_{i \in [n]} \left(G(d_i)^\top (f(q_i) - F(q_i)) \left(1 - \sigma(F(q_i)^\top G(d_i)) \right) + \gamma(-f(q_i)^\top G(d_i)) - \gamma(-F(q_i)^\top G(d_i)) \right) \\
&\leq \frac{1}{n} \sum_{i \in [n]} \left(\|G(d_i)\| \|f(q_i) - F(q_i)\| + \left| f(q_i)^\top G(d_i) - F(q_i)^\top G(d_i) \right| \right) \\
&\leq \frac{2K}{n} \sum_{i \in [n]} \|f(q_i) - F(q_i)\|_2.
\end{aligned} \tag{22}$$

\square_3 can be bounded as

$$\begin{aligned}
\square_3 &= R(s^{F,G}, s^{F,G}; \mathcal{S}_n) - R(s^{F,G}; \mathcal{S}_n) \\
&= \frac{1}{n} \sum_{i \in [n]} \left(\ell_d(s^{F,G}(q_i, d_i), s^{F,G}(q_i, d_i)) - \ell(s^{F,G}(q_i, d_i), y_i) \right) \\
&= \frac{1}{n} \sum_{i \in [n]} \left(\left(1 - \sigma(F(q_i)^\top G(d_i)) \right) F(q_i)^\top G(d_i) + \gamma(-F(q_i)^\top G(d_i)) \right. \\
&\quad \left. - (1 - y_i) F(q_i)^\top G(d_i) - \gamma(-F(q_i)^\top G(d_i)) \right)
\end{aligned}$$

$$\begin{aligned}
&= \frac{1}{n} \sum_{i \in [n]} \left((1 - \sigma(F(q_i)^\top G(d_i))) - (1 - y_i) \right) F(q_i)^\top G(d_i) \\
&\leq \frac{K^2}{n} \sum_{i \in [n]} \left| \sigma(F(q_i)^\top G(d_i)) - y_i \right|. \tag{23}
\end{aligned}$$

Combining Eq. 20, 21, 22, and 23 establishes the bound in Eq. 17. \square

Lemma C.3. *Given an example $(q, d, y) \in \mathcal{Q} \times \mathcal{D} \times \{0, 1\}$, let $s^{f,g}(q, d) = f(q)^\top g(d)$ be the scores assigned to the (q, d) pair by a dual-encoder model with f and g as query and document encoders, respectively. Let ℓ and ℓ_d be the binary cross-entropy loss (cf. Eq. 9 with $L = 1$) and the distillation-specific loss based on it (cf. Eq. 11 with $L = 1$), respectively. In particular,*

$$\begin{aligned}
\ell(s^{f,g}(q, d), y) &:= -y \log \sigma(f(q)^\top g(d)) - (1 - y) \log [1 - \sigma(f(q)^\top g(d))] \\
\ell_d(s^{f,g}(q, d), s^{F,G}(q, d)) &:= -\sigma(F(q)^\top G(d)) \cdot \log \sigma(f(q)^\top g(d)) - \\
&\quad [1 - \sigma(F(q)^\top G(d))] \cdot \log [1 - \sigma(f(q)^\top g(d))],
\end{aligned}$$

where σ is the sigmoid function and $s^{F,G}$ denotes the teacher dual-encoder model with F and G as its query and document encoders, respectively. Assume that

1. All encoders f, g, F , and G have the same output dimension $k \geq 1$.
2. $\exists K \in (0, \infty)$ such that

$$\sup_{q \in \mathcal{Q}} \max \{ \|f(q)\|_2, \|F(q)\|_2 \} \leq K$$

and

$$\sup_{d \in \mathcal{D}} \max \{ \|g(d)\|_2, \|G(d)\|_2 \} \leq K.$$

Then, we have

$$\underbrace{\mathbb{E}[\ell(s^{f,g}(q, d), y)]}_{:= R(s^{f,g})} - \underbrace{\mathbb{E}[\ell_d(s^{f,g}(q, d), s^{F,G}(q, d))]}_{:= R(s^{f,g}, s^{F,G})} \leq K_Q K_D \mathbb{E} \left[\left| \sigma(F(q)^\top G(d)) - y \right| \right] \tag{24}$$

where expectation are defined by a joint distribution $\mathbb{P}(q, d, y)$ over $\mathcal{Q} \times \mathcal{D} \times \{0, 1\}$

Proof. Similar to the proof of Proposition C.2, we utilize the fact that

$$\begin{aligned}
\ell(s^{F,G}(q, d), y) &= (1 - y) F(q)^\top G(d) + \gamma(-F(q)^\top G(d)), \\
\ell_d(s^{f,g}(q, d), s^{F,G}(q, d)) &= \left(1 - \sigma(F(q)^\top G(d)) \right) f(q)^\top g(d) + \gamma(-f(q)^\top g(d)),
\end{aligned}$$

where $\gamma(v) := \log[1 + e^v]$ is the softplus function. Now,

$$\begin{aligned}
&\mathbb{E} \left[\ell(s^{f,g}(q, d), y) - \ell_d(s^{f,g}(q, d), s^{F,G}(q, d)) \right] \\
&= \mathbb{E} \left[(1 - y) f(q)^\top g(d) + \gamma(-f(q)^\top g(d)) \right] \\
&\quad - \mathbb{E} \left[\left(1 - \sigma(F(q)^\top G(d)) \right) f(q)^\top g(d) + \gamma(-f(q)^\top g(d)) \right] \tag{25}
\end{aligned}$$

$$\begin{aligned}
&= \mathbb{E} \left[\left(1 - y - (1 - \sigma(F(q)^\top G(d))) \right) F(q)^\top G(d) \right] \\
&\leq K^2 \mathbb{E} \left[\left| \sigma(F(q)^\top G(d)) - y \right| \right], \tag{26}
\end{aligned}$$

which completes the proof. \square

C.2 Uniform deviation bound

Let \mathcal{F} denote the class of functions that map queries in \mathcal{Q} to their embeddings in \mathbb{R}^k via the query encoder. Define \mathcal{G} analogously for the doc encoder, which consists of functions that map documents in \mathcal{D} to their embeddings in \mathbb{R}^k . To simplify exposition, we assume that each training example consists of a single relevant or irrelevant document for each query, i.e., $L = 1$ in Section 3. Let

$$\mathcal{FG} = \{(q, d) \mapsto f(q)^\top g(d) \mid f \in \mathcal{F}, g \in \mathcal{G}\}$$

Given $\mathcal{S}_n = \{(q_i, d_i, y_i) : i \in [n]\}$, let $N(\epsilon, \mathcal{H})$ denote the ϵ -covering number of a function class \mathcal{H} with respect to $L_2(\mathbb{P}_n)$ norm, where $\|h\|_{L_2(\mathbb{P}_n)}^2 := \|h\|_n^2 := \frac{1}{n} \sum_{i=1}^n \|h(q_i, d_i)\|_2^2$. Depending on the context, the functions in \mathcal{H} may map to \mathbb{R} or \mathbb{R}^d .

Proposition C.4. *Let s^t be scorer of a teacher model and ℓ_d be a distillation loss function which is L_{ℓ_d} -Lipschitz in its first argument. Let the embedding functions in \mathcal{F} and \mathcal{G} output vectors with ℓ_2 norms at most K . Define the uniform deviation*

$$\mathcal{E}_n(\mathcal{F}, \mathcal{G}) = \sup_{f \in \mathcal{F}, g \in \mathcal{G}} \left| \frac{1}{n} \sum_{i \in [n]} \ell_d(f(q_i)^\top g(d_i), s_{q_i, d_i}^t) - \mathbb{E}_{q, d} \ell_d(f(q)^\top g(d), s_{q, d}^t) \right|.$$

For any $g^* \in \mathcal{G}$, we have

$$\begin{aligned}
\mathbb{E}_{\mathcal{S}_n} \mathcal{E}_n(\mathcal{F}, \mathcal{G}) &\leq \mathbb{E}_{\mathcal{S}_n} \frac{48KL_{\ell_d}}{\sqrt{n}} \int_0^\infty \sqrt{\log N(u, \mathcal{F}) + \log N(u, \mathcal{G})} du, \\
\mathbb{E}_{\mathcal{S}_n} \mathcal{E}_n(\mathcal{F}, \{g^*\}) &\leq \mathbb{E}_{\mathcal{S}_n} \frac{48KL_{\ell_d}}{\sqrt{n}} \int_0^\infty \sqrt{\log N(u, \mathcal{F})} du.
\end{aligned}$$

Proof of Proposition C.4. We first symmetrize excess risk to get Rademacher complexity, then bound the Rademacher complexity with Dudley's entropy integral.

For a training set \mathcal{S}_n , the empirical Rademacher complexity of a class of functions \mathcal{H} that maps $\mathcal{Q} \times \mathcal{D}$ to \mathbb{R} is defined by

$$\text{Rad}_n(\mathcal{H}) = \mathbb{E}_\sigma \sup_{h \in \mathcal{H}} \frac{1}{n} \sum_{i=1}^n \varepsilon_i h(q_i, d_i),$$

where $\{\varepsilon_i\}$ denote i.i.d. Rademacher random variables taking the value in $\{+1, -1\}$ with equal probability. By symmetrization [Bousquet et al., 2004] and the fact that ℓ_d is L_{ℓ_d} -Lipschitz in its first argument, we get

$$E_{\mathcal{S}_n} \mathcal{E}_n(\mathcal{F}, \mathcal{G}) \leq 2L_{\ell_d} \mathbb{E}_{\mathcal{S}_n} \text{Rad}_n(\mathcal{FG}).$$

Then, Dudley's entropy integral [see, e.g., Ledoux and Talagrand, 1991] gives

$$\text{Rad}_n(\mathcal{FG}) \leq \frac{12}{\sqrt{n}} \int_0^\infty \sqrt{\log N(u, \mathcal{FG})} du.$$

From Lemma C.5 with $K_Q = K_D = K$, for any $u > 0$,

$$N(u, \mathcal{FG}) \leq N\left(\frac{u}{2K}, \mathcal{F}\right) N\left(\frac{u}{2K}, \mathcal{G}\right).$$

Putting these together,

$$\mathbb{E}_{\mathcal{S}_n} \mathcal{E}_n(\mathcal{F}, \mathcal{G}) \leq \frac{24L_{\ell_d}}{\sqrt{n}} \int_0^\infty \sqrt{\log N(u/2K, \mathcal{F}) + \log N(u/2K, \mathcal{G})} du. \quad (27)$$

Following the same steps with \mathcal{G} replaced by $\{g^*\}$, we get

$$\mathbb{E}_{\mathcal{S}_n} \mathcal{E}_n(\mathcal{F}, \{g^*\}) \leq \frac{24L_{\ell_d}}{\sqrt{n}} \int_0^\infty \sqrt{\log N(u/2K, \mathcal{F})} du \quad (28)$$

By changing variable in Eq. 27 and Eq. 28, we get the stated bounds. \square

For $f : \mathcal{Q} \rightarrow \mathbb{R}^k, g : \mathcal{D} \rightarrow \mathbb{R}^k$, define $fg : \mathcal{Q} \times \mathcal{D} \rightarrow \mathbb{R}$ by $fg(q, d) = f(q)^\top g(d)$.

Lemma C.5. *Let f_1, \dots, f_N be an ϵ -cover of \mathcal{F} and g_1, \dots, g_M be an ϵ -cover of \mathcal{G} in $L_2(\mathbb{P}_n)$ norm. Let $\sup_{f \in \mathcal{F}} \sup_{q \in \mathcal{Q}} \|f(q)\|_2 \leq K_Q$ and $\sup_{g \in \mathcal{G}} \sup_{d \in \mathcal{D}} \|g(d)\|_2 \leq K_D$. Then,*

$$\{f_i g_j \mid i \in [N], j \in [M]\}$$

is a $(K_Q + K_D)\epsilon$ -cover of \mathcal{FG} .

Proof of Lemma C.5. For arbitrary $f \in \mathcal{F}, g \in \mathcal{G}$, there exist $\tilde{f} \in \{f_1, \dots, f_N\}, \tilde{g} \in \{g_1, \dots, g_M\}$ such that $\|f - \tilde{f}\|_n \leq \epsilon, \|g - \tilde{g}\|_n \leq \epsilon$. It is sufficient to show that $\|fg - \tilde{f}\tilde{g}\|_n \leq (K_Q + K_D)\epsilon$. Decomposing using triangle inequality,

$$\begin{aligned} \|fg - \tilde{f}\tilde{g}\|_n &= \|fg - f\tilde{g} + f\tilde{g} - \tilde{f}\tilde{g}\|_n \\ &\leq \|fg - f\tilde{g}\|_n + \|f\tilde{g} - \tilde{f}\tilde{g}\|_n. \end{aligned} \quad (29)$$

To bound the first term, using Cauchy-Schwartz inequality, we can write

$$\frac{1}{n} \sum_{i=1}^n \left(f(q_i)^\top g(d_i) - \tilde{f}(q_i)^\top \tilde{g}(d_i) \right)^2 \leq \sup_{q \in \mathcal{Q}} \|f(q)\|_2^2 \cdot \frac{1}{n} \sum_{i=1}^n \|(g - \tilde{g})(d_i)\|_2^2.$$

Therefore

$$\|fg - f\tilde{g}\|_n \leq K_Q \|g - \tilde{g}\|_n \leq K_Q \epsilon.$$

Similarly

$$\|f\tilde{g} - \tilde{f}\tilde{g}\|_n \leq K_D \|f - \tilde{f}\|_n \leq K_D \epsilon$$

Plugging these in Eq. 29, we get

$$\|fg - \tilde{f}\tilde{g}\|_n \leq (K_Q + K_D)\epsilon.$$

This completes the proof. \square

D Evaluation metric details

For NQ, we evaluate models with full *strict* recall metric, meaning that the model is required to find a *golden* passage from the whole set of candidates (21M). Specifically, for $k \geq 1$, $\text{recall}@k$ or $\text{R}@k$ denotes the percentage of questions for which the associated golden passage is among the k passages that receive the highest relevance scores by the model. In addition, we also present results for *relaxed* recall metric considered by Karpukhin et al. [2020a], where $\text{R}@k$ denotes the percentage of questions where the corresponding answer string is present in at least one of the k passages with the highest model (relevance) scores.

For both MSMARCO retrieval and re-ranking tasks, we follow the standard evaluation metrics *Mean Reciprocal Rank*(MRR)@10 and *normalized Discounted Cumulative Gain* (nDCG)@10. For retrieval tasks, these metrics are computed with respect to the whole set of candidates passages (8.8M). On the other hand, for re-ranking task, the metrics are computed with respect to BM25 generated 1000 candidate passages for each query. We report $100 \times \text{MRR}@10$ and $100 \times \text{nDCG}@10$, as per the convention followed in the prior works.

E Query generation details

We introduced query generation to encourage geometric matching in local regions, which can aid in transferring more knowledge in confusing neighborhoods. As expected, this further improves the distillation effectiveness on top of the embedding matching in most cases. To focus on the local regions, we generate queries from the observed examples by adding local perturbation in the data manifold (embedding space). Specifically, we employ an off-the-shelf encoder-decoder model – BART-base Lewis et al. [2020]. First, we embed an observed query in the corresponding dataset. Second, we add a small perturbation to the query embedding. Finally, we decode the perturbed embedding to generate a new query in the input space. Formally, the generated query x' given an original query x takes the form $x' = \text{Dec}(\text{Enc}(x) + \epsilon)$, where $\text{Enc}()$ and $\text{Dec}()$ correspond to the encoder and the decoder from the off-the-shelf model, respectively, and ϵ is an isotropic Gaussian noise. Furthermore, we also randomly mask the original query tokens with a small probability. We generate two new queries from an observed query and use them as additional data points during our distillation procedure.

As a comparison, we tried adding the same size of random sampled queries instead of the ones generated via the method described above. That did not show any benefit, which justifies the use of our query/question generation method.

F Experimental details and additional results

F.1 Additional training details

Optimization. For all of our experiments, we use ADAM weight decay optimizer with a short warm up period and a linear decay schedule. We use the initial learning rate of 10^{-5} and 2.8×10^{-5} for experiments on NQ and MSMARCO, respectively. The batch sizes is 128.

F.2 Additional results on NQ

See Table 7 for the performance of various DE models on NQ, as measured by the *relaxed* recall metric.

Table 7: *Relaxed* recall performance of various student DE models on NQ dev set, including symmetric DE student model (67.5M or 11.3M transformer for both encoders), and asymmetric DE student model (67.5M or 11.3M transformer as query encoder and document embeddings inherited from the teacher). All distilled students used the same teacher (110M parameter BERT-base models as both encoders), with the performance (in terms of relaxed recall) of Recall@5 = 87.2, Recall@20 = 94.7, Recall@100 = 98.1. *Note: the proposed method can achieve 100% of teacher’s performance even with 2/3rd size of the query encoder, and 92-97% with even 1/8th size.*

Method	Recall@5		Recall@20		Recall@100	
	67.5M	11.3M	67.5M	11.3M	67.5M	11.3M
Train student directly	62.5	49.7	82.5	73.0	93.7	88.2
+ Distill from teacher	82.7	66.1	92.9	84.0	97.3	93.1
+ Inherit document embeddings	84.7	73.0	93.7	85.4	97.6	93.3
+ Query embedding matching	87.2	77.6	95.0	88.0	97.9	94.3
+ Query generation	87.8	80.3	94.8	89.9	98.0	95.6
Train student only using embedding matching and inherit doc embeddings	86.4	69.1	94.2	81.6	97.7	89.9
+ Query generation	86.7	72.9	94.4	84.9	97.8	92.2

F.3 Additional results on MSMARCO

See Table 8 for CE to DE distillation results on MSMARCO re-ranking task, as measured by the nDCG@10 metric.

Table 8: Performance of CE to DE distillation on MSMARCO re-ranking task, as measured by the nDCG@10 metric. As for the teacher CE models, we consider two kinds of CE models based on two different pooling mechanism.

Method	nDCG@10
[CLS] -pooled teacher	43.0
Dual-pooled teacher	42.8
Standard distillation from [CLS] -teacher	38.8
+Joint matching	38.0
Standard distillation from Dual-pooling teacher	39.2
+Query matching	39.4

F.4 Additional results on BEIR benchmark

See Table 9 (NDCG@10) and Table 10 (Recall@100) for BEIR benchmark results. All numbers are from BEIR benchmark paper [Thakur et al., 2021]. As common practice, non-public benchmark sets⁸, {BioASQ, Signal-1M(RT), TREC-NEWS, Robust04}, are removed from the table. Following the original BEIR paper [Thakur et al., 2021] (Table 9 and Appendix G from the original paper), we utilized Capped Recall@100 for TREC-COVID dataset.

Table 9: In-domain and zero-shot retrieval performance on BEIR benchmark [Thakur et al., 2021], as measured by **nDCG@10**. All the baseline number in the table are taken from Thakur et al. [2021]. We exclude (in-domain) MSMARCO from average computation as common practice.

Model (→)	Lexical				Sparse					Dense			
					BM25	DeepCT	SPARTA	docT5query	DPR	ANCE	TAS-B	GenQ	SentenceBERT (our teacher)
MS MARCO	22.8	29.6 [‡]	35.1 [‡]	33.8 [‡]	17.7	38.8 [‡]	40.8 [‡]	40.8 [‡]	47.1 [‡]			46.6 [‡]	
TREC-COVID	65.6	40.6	53.8	71.3	33.2	65.4	48.1	61.9	75.4			72.3	
NFCorpus	32.5	28.3	30.1	32.8	18.9	23.7	31.9	31.9	31.0			30.7	
NQ	32.9	18.8	39.8	39.9	47.4 [‡]	44.6	46.3	35.8	51.5			50.8	
HotpotQA	60.3	50.3	49.2	58.0	39.1	45.6	58.4	53.4	58.0			56.0	
FiQA-2018	23.6	19.1	19.8	29.1	11.2	29.5	30.0	30.8	31.8			29.5	
ArguAna	31.5	30.9	27.9	34.9	17.5	41.5	42.9	49.3	38.5			34.9	
Touché-2020	36.7	15.6	17.5	34.7	13.1	24.0	16.2	18.2	22.9			24.7	
CQADupStack	29.9	26.8	25.7	32.5	15.3	29.6	31.4	34.7	33.5			30.6	
Quora	78.9	69.1	63.0	80.2	24.8	85.2	83.5	83.0	84.2			81.4	
DBpedia	31.3	17.7	31.4	33.1	26.3	28.1	38.4	32.8	37.7			35.9	
SCIDOCs	15.8	12.4	12.6	16.2	07.7	12.2	14.9	14.3	14.8			14.4	
FEVER	75.3	35.3	59.6	71.4	56.2	66.9	70.0	66.9	76.7			76.9	
Climate-FEVER	21.3	06.6	08.2	20.1	14.8	19.8	22.8	17.5	23.5			22.5	
SciFact	66.5	63.0	58.2	67.5	31.8	50.7	64.3	64.4	59.8			55.5	
AVG (w/o MSMARCO)	43.0	31.0	35.5	44.4	25.5	40.5	42.8	42.5	45.7			44.0	

Table 10: In-domain and zero-shot retrieval performance on BEIR benchmark [Thakur et al., 2021], as measured by **Recall@100**. All the baseline number in the table are taken from Thakur et al. [2021]. [‡] indicates in-domain retrieval performance. * indicates capped recall following original benchmark setup. We exclude (in-domain) MSMARCO from average computation as common practice.

Model (→)	Lexical				Sparse					Dense			
					BM25	DeepCT	SPARTA	docT5query	DPR	ANCE	TAS-B	GenQ	SentenceBERT (our teacher)
MS MARCO	65.8	75.2 [‡]	79.3 [‡]	81.9 [‡]	55.2	85.2 [‡]	88.4 [‡]	88.4 [‡]	91.7 [‡]			90.6 [‡]	
TREC-COVID	49.8*	34.7*	40.9*	54.1*	21.2*	45.7*	38.7*	45.6*	54.1*			48.8*	
NFCorpus	25.0	23.5	24.3	25.3	20.8	23.2	28.0	28.0	27.7			26.7	
NQ	76.0	63.6	78.7	83.2	88.0 [‡]	83.6	90.3	86.2	91.1			89.9	
HotpotQA	74.0	73.1	65.1	70.9	59.1	57.8	72.8	67.3	69.7			68.3	
FiQA-2018	53.9	48.9	44.6	59.8	34.2	58.1	59.3	61.8	62.0			60.1	
ArguAna	94.2	93.2	89.3	97.2	75.1	93.7	94.2	97.8	89.2			87.8	
Touché-2020	53.8	40.6	38.1	55.7	30.1	45.8	43.1	45.1	45.3			45.5	
CQADupStack	60.6	54.5	52.1	63.8	40.3	57.9	62.2	65.4	63.9			61.3	
Quora	97.3	95.4	89.6	98.2	47.0	98.7	98.6	98.8	98.5			98.1	
DBpedia	39.8	37.2	41.1	36.5	34.9	31.9	49.9	43.1	46.0			42.6	
SCIDOCs	35.6	31.4	29.7	36.0	21.9	26.9	33.5	33.2	32.5			31.5	
FEVER	93.1	73.5	84.3	91.6	84.0	90.0	93.7	92.8	93.9			93.8	
Climate-FEVER	43.6	23.2	22.7	42.7	39.0	44.5	53.4	45.0	49.3			47.6	
SciFact	90.8	89.3	86.3	91.4	72.7	81.6	89.1	89.3	88.9			87.2	
AVG (w/o MSMARCO)	63.4	55.9	56.2	64.7	47.7	60.0	64.8	64.2	65.1			63.5	

⁸<https://github.com/beir-cellard/beir>

F.5 Additional results with single-stage trained teachers

Hereby we evaluate EmbedDistill with a simple single-stage trained teachers instead of teachers trained in complex multi-stage frameworks, in order to test the generalizability of the method.

Similar to Table 1, we conducted an experiment on top of single-stage trained teacher based on RoBERTa-base instead of AR2 [Zhang et al., 2022] in the main text. We also changed the student to be based on DistilRoBERTa or RoBERTa-mini accordingly for simplicity to use same tokenizer.

Table 11 demonstrates that EmbedDistill provides a significant boost of the performance on top of standard distillation techniques similar to what we observed in Table 1.

Table 11: *Full* recall performance of various student DE models on NQ dev set, including symmetric DE student model, and asymmetric DE student models. All students used the same *in-house teacher* (124M parameter RoBERTa-base models as both encoders), with the full Recall@5 = 64.6, Recall@20 = 81.7, and Recall@100 = 91.5.

Method	6-Layer (82M)			4-Layer (16M)		
	R@5	R@20	R@100	R@5	R@20	R@100
Train student directly	41.9	64.5	82.0	39.5	59.9	76.3
+ Distill from teacher	48.3	67.2	80.9	44.9	61.1	74.8
+ Inherit doc embeddings	56.9	74.3	85.4	47.2	64.0	77.0
+ Query embedding matching	61.8	78.7	89.0	56.7	74.6	85.9
+ Query generation	61.7	79.4	89.6	57.1	75.2	86.7
Train student using only embedding matching and inherit doc embeddings	63.7	80.3	90.3	57.9	74.6	85.7
+ Query generation	64.1	80.5	90.4	58.9	76.0	86.6

Furthermore, we also consider a in-house trained teacher (RoBERTa-base) for MSMARCO reranking task. Table 12 demonstrates a similar pattern to Table 3, providing evidence of generalizability of EmbedDistill.

Table 12: Reranking performance of various DE models on MSMARCO dev set. We utilize a RoBERTa-base in-house trained teacher achieving MRR@10 of 33.1 and nDCG@10 of 38.8 is used. The table shows performance of the symmetric DE student model and asymmetric DE student models.

Method	MRR@10		nDCG@10	
	82M	16M	82M	16M
Train student directly	29.7	26.3	35.2	31.4
+ Distill from teacher	31.6	28.4	37.2	33.5
+ Inherit doc embeddings	32.4	30.2	38.0	35.8
+ Query embedding matching	32.8	31.9	38.6	37.6
+ Query generation	33.0	32.0	38.8	37.7
Train student only using embedding matching and inherit doc embeddings	32.7	31.8	38.5	37.5
+ Query generation	33.0	31.8	38.9	37.5

These result showcase that our method brings performance boost orthogonal to how teacher was trained, whether single-staged or multi-staged.

G Embedding analysis

G.1 DE to DE distillation

Traditional score matching-based distillation might not result in transfer of relative geometry from teacher to student. To assess this, we look at the discrepancy between the teacher and student query embeddings for all q, q' pairs: $\|\mathbf{emb}_q^t - \mathbf{emb}_{q'}^t\| - \|\mathbf{emb}_q^s - \mathbf{emb}_{q'}^s\|$. Note that the analysis is based on NQ, and we focus on the teacher and student DE models based on BERT-base and DistilBERT, respectively. As evident from Fig. 4, embedding matching loss significantly reduces this discrepancy.

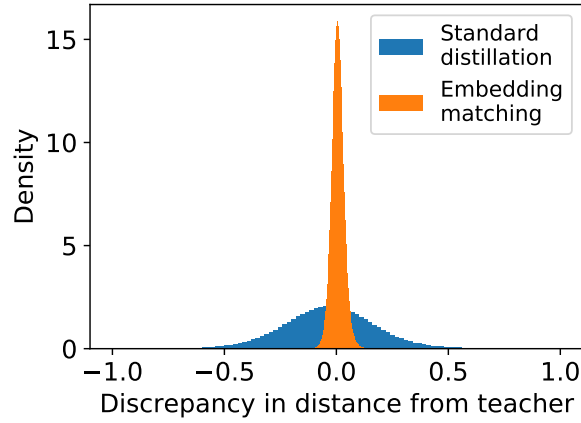


Figure 4: Histogram of teacher-student distance discrepancy in queries.

G.2 CE to DE distillation

We qualitatively look at embeddings from CE model in Fig. 5. The embedding $\mathbf{emb}_{q,d}^t$ from [CLS]-pooled CE model does not capture semantic similarity between query and document as it is solely trained to classify whether the query-document pair is relevant or not. In contrast, the (proxy) query embeddings $\mathbf{emb}_{q \leftarrow (q,d)}^t$ from our Dual-pooled CE model with reconstruction loss do not degenerate and its embeddings groups same query whether conditioned on positive or negative document together. Furthermore, other related queries are closer than unrelated queries. Such informative embedding space would aid distillation to a DE model via embedding matching.

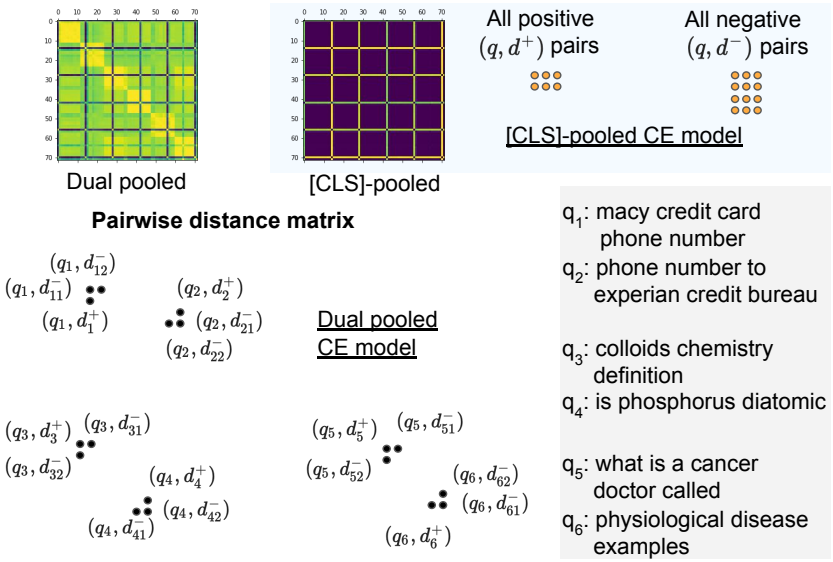


Figure 5: Illustration of geometry expressed by [CLS]-pooled CE and our Dual-pooled CE model on 6 queries from MSMARCO and 12 passages based on pairwise distance matrix across these 72 pairs. [CLS]-pooled CE embeddings degenerates as all positive and negative query-document pairs almost collapse to two points and fail to capture semantic information. In contrast, our Dual-pooled CE model leads to much richer representation that can express semantic information.